Environmental analogs from yellowstone hot springs on geochemical and microbial diversity with implications for the search for life on Mars

D Boulesteix, A Buch, G Masson, L L Kivrak, J R Havig, T L Hamilton, B L Teece, Y He, Caroline Freissinet, Y Huang, et al.

Planetary and Space Science 250 (2024) 105953

Contents lists available at ScienceDirect

Planetary and Space Science

journal homepage: www.elsevier.com/locate/pss

Environmental analogs from yellowstone hot springs on geochemical and microbial diversity with implications for the search for life on Mars

D. Boulesteix [a,*], A. Buch [a], G. Masson [a], L.L. Kivrak [b], J.R. Havig [c,d], T.L. Hamilton [c,e], B.L. Teece [f], Y. He [g], C. Freissinet [h], Y. Huang [i], E. Santos [i], C. Szopa [h], A.J. Williams [b]

[a] Laboratoire Génie des Procédés et Matériaux, CentraleSupélec, University Paris-Saclay, 8-10 rue Joliot-Curie, 91190, Gif-sur-Yvette, France
[b] Department of Geological Sciences, University of Florida, Gainesville, FL 32611, USA
[c] Dept. of Plant and Microbial Biology, University of Minnesota, St. Paul, MN, 55108, USA
[d] Dept. of Earth and Environmental Sciences, University of Minnesota, Minneapolis, MN 55455, USA
[e] The BioTechnology Institute, University of Minnesota, St. Paul, MN 55108, USA
[f] NASA Jet Propulsion Laboratory, California Institute of Technology, Pasadena, CA, USA
[g] Institut de Minéralogie, de Physique des Matériaux et de Cosmochimie, Sorbonne Université - CNRS, MNHN, France
[h] LATMOS/IPSL, UVSQ University Paris-Saclay, Sorbonne University, CNRS, 11 Bd d'Alembert, 78280, Guyancourt, France
[i] Department of Geological Sciences, Brown University, 324 Brook Street, Providence, RI 02912, USA

ARTICLE INFO

Keywords:
Perseverance rover
Metabolomics
Mars
Hot springs
Terrestrial analogs
Agnostic and gnostic signatures

ABSTRACT

From Viking landers to Perseverance rover, Mars has been explored by several *in situ* missions capable of analyzing organic compounds. Results from the SAM and SHERLOC on Curiosity and Perseverance, respectively, support the detection of lean organic matter (at ppb-ppm levels) in the top surface samples, although the source (s) and preservation mechanisms are still ambiguous. Perseverance is currently exploring a fluvio-lacustrine system at Jezero crater and may explore an ancient volcanic terrain after exiting the crater. As Perseverance would collect samples for potential return to Earth, preparation is needed for sample return efforts through various means including i) the detection of trace organic compounds in various matrices, ii) validation of compounds identified by Martian rovers, and iii) better understanding of mechanisms of their production on Mars. On these returned samples, the community may be able to resolve the timing of organic matter formation and refine hypotheses regarding organic preservation in Martian soils despite the presence of numerous oxidants, salts, and pH-temperature intra and inter-site variations that are less conductive to long-term preservation of organic matter. For instance, acidic conditions promote clay catalyzed isomerization, but seem to benefit for the fatty acid preservation producing organic-salts or favoring salt dissolution in the matrix to protect organic compounds from radiations and water alteration. With a similar aim, we selected samples from Yellowstone National Park hot springs and silica sinters as analogs to locations visited by Curiosity and Perseverance or – in the future – Rosalind Franklin rover. The hot springs in this study developed over hundreds to thousands of years, providing optimal conditions (*i.e.,* matrix composition, temperature, pH) of preservation for organic molecules, extremophilic and mesophilic cells. In our study, the most well preserved organic matter and biosignatures were detected in acidic silica sinters with a surface (water) temperature below 50 °C and a minor crystalline phase. The gas chromatography – mass spectrometry molecular analysis revealed a variety of organic compounds we classified as bioindicators (such as amino acids, nucleobases, and sugars), and biosignatures (such as long-chain branched and/or (poly)unsaturated lipids, secondary metabolites involved in the quorum sensing or communication between individuals). We validated with a SAM/MOMA-like benchtop extracting oven the organic matter extraction protocols performed with the SAM experiment. We identified using the different SAM and MOMA extraction protocols (pyrolysis and wet-chemistry derivatizations) eight microbial classes through a unique untargeted environmental metabolomics' method embracing space flight technology constraints. Additionally, we identified one (and likely two) agnostic biosignature(s): i) the concomitance of some elements and organic compounds in the analogs (correlation of organic matter elements: C, N, S, P and organic molecules co-located with essential biological elements: Fe, Mg, V, Mn and non-essential biological elements concentrated by

* Corresponding author.
E-mail address: david.boulesteix@centralesupelec.fr (D. Boulesteix).

https://doi.org/10.1016/j.pss.2024.105953
Received 8 March 2024; Received in revised form 26 July 2024; Accepted 8 August 2024
Available online 10 August 2024

microorganisms: As, Cs, Ga), and ii) the negative isotope C and N ratio demonstrating organic molecules rich in ^{12}C and ^{14}N: archaeal, bacterial, and eukaryotic lipids for an efficient low energy-consuming metabolism.

1. Introduction

a. Exploration of Mars surface and subsurface environments

Mars exploration has leveraged increasingly sophisticated robotics with improving analytical capabilities, since the first landers (Viking I and II, 1976) and rovers (Mars Exploration Rover, Sojourner, Mars Pathfinder Mission, 1997), and culminating in the current Curiosity (Mars Science Laboratory Mission – MSL, 2012) and Perseverance (Mars, 2020 Mission, 2021) rovers. The types of flight-ready analytical capabilities to search for traces of life have expanded from the initial cameras and infrared (IR) spectrometers in Viking landers-orbiters to a wider range of spectroscopy analyzers. In addition to infrared and ultraviolet (UV) spectrometers, nowadays, the onboard rovers' analytical suit of instruments comprise Raman spectrometers analyzing inorganic and organic matter, including the latest deep ultraviolet laser excitation onboard the Perseverance Raman Scanning Habitable Environments with Raman and Luminescence for Organics and Chemicals (SHERLOC) instrument (Hays et al., 2017; Corpolongo et al., 2023; Hays, 2015). Analytical payloads also carry mass spectrometers to analyze the bulk elemental composition of organic matter, the isotopic fractionation, and proceed up to the molecular identification (Biemann, 2007; Palmer and Limero, 2001; Klein et al., 1976). The mass spectrometers have the longest heritage, with the Viking landers (Biemann et al., 1977), followed by the Phoenix polar lander (Boynton et al., 2001), and the latest landed mass spectrometer in the Sample Analysis at Mars (SAM) from the MSL mission onboard the Curiosity rover (Mahaffy et al., 2012).

Each mission has explored different formations with potentially preserved organic compounds for hundreds of millions to billions of years (François et al., 2016) from harsh surface conditions, including drastic changes in temperature, pressure, and oxidative content of the atmosphere and soils submitted to energetic solar and galactic radiative particles or photons (Hassler et al., 2014a; Kminek and Bada, 2006; Pavlov et al., 2012). Since 2012, the Curiosity rover has explored the 3.5–3.7 Ga Gale Crater, observing hyper-arid and evaporitic clay basins (Grotzinger et al., 2012; Grotzinger and Al-Rawahi, 2014; L'Haridon et al., 2020) rich in silica (*e.g.,* Opal-A SiO_2) and different salts/minerals, such as calcium perchlorate (especially in Yellowknife bay) (Carrier and Kounaves, 2015; Clark and Kounaves, 2016), and magnesium sulfate (Mount Sharp) (Aubrey et al., 2006; Lewis et al., 2015). These hyper-arid environments favor subsurface xero-preservation and protective organo-mineral interactions along with UV shielding as numerous studies observed on Earth analogs including the Atacama Mars analog where fossilized cells are well preserved (Casero et al., 2021; Crits-Christoph et al., 2013; Navarro-Gonzalez, 2003; Wilhelm et al., 2017).

Since 2021, the Perseverance rover has explored Jezero Crater, which contains deposits with Fe/Mg-smectites, other clay minerals, and sediments deposited by water around 3.5–3.6 Ga (Scheller et al., 2022; Mangold et al., 2020; Goudge et al., 2017; Stack-Morgan et al., 2023). The depositional history of Jezero was initially interpreted to be a delta (Scheller et al., 2022; Mangold et al., 2020) similar to the Mississippi delta river in the USA (Schon et al., 2012). However, after recent Perseverance investigations, the site may be better defined as a deltaic fan since the sedimentary deposit characteristics are not specific to being a delta or an alluvial fan (Scheller et al., 2022). Near the Octavia E. Butler landing site at Jezero Crater, volcanic activity from NE Syrtis (on the western edge of Isidis Planitia plain) introduced mafic volcanic units that served as a source of remnant olivine-bearing carbonate rocks. These deposits and rocks have the potential to be linked to biotic past traces, such as microbial deposits with concentrated nutrients and light elements' depletion in sediments or a low erosion rate allowing (bio) signatures xero-preservations in this unique olivine-bearing unit (Mangold et al., 2020; Goudge et al., 2017) that harbors a wide array of observed mineralogical and organo-mineral complexes (Wilhelm et al., 2017; Stack-Morgan et al., 2023). The SHERLOC instrument has been used to identify pyroxene (at Dourbes), sulfate (at Quartier), and perchlorate (at Guillaumes) salts within the low silica and rich olivine matrix, as well as predominantly silica samples relatively free from salt (*e.g.,* Alfalfa) (Corpolongo et al., 2023). The carbonate and silica samples collected are thought to be high value targets for detecting traces of life and diverse organic compounds due to the presence of organo-mineral formations that have a high potential to encapsulate organic materials and protect them from the harsh Mars surface environment, such as sulfates or sulfur-bearing layers, clays and silica sinters or sediments (Casero et al., 2021; Navarro-Gonzalez, 2003; Eigenbrode et al., 2018; Gainey et al., 2017; Pancost et al., 2005).

The planned Rosalind Franklin rover from the ESA-led ExoMars 2028 mission would explore the clay-rich Oxia Planum region (Sharma et al., 2023; Goesmann et al., 2017; Fawdon et al., 2024). The rover's payload will include the Mars Organic Molecule Analyser (MOMA) (Alwmark et al., 2023; Brown et al., 2020), a laser desorption ionization and a gas chromatograph, coupled to a dual-entry mass spectrometer (GC-MS). One drill will perform a hole up to 2 m, and GC-MS analyses, for the first time, will be done on Mars subsurface samples. In addition to the MOMA instrument, the Rosalind Franklin rover would embark three other instruments in the Analytical Laboratory Drawer (ALD) able to detect organic matter, namely the Mars Multispectral Imager for Subsurface Studies (Ma_MISS) embedded in the drill tip (Ferrari et al., 2023), the MicrOmega (Bibring et al., 2017), and the Raman Laser Spectrometer (RLS) (Vago et al., 2017; Veneranda et al., 2021). Results from these future analyses will bring new insight about organic matter preservation in Martian deep layers that are not impacted by UV and primary X-rays. Secondary X-rays and stronger energy sources like gamma and cosmic/energetic particles' radiations reach the first few meters, but with a lower incident energy than within the first centimeters of the Martian regolith. These destructive processes explain the low detection of organic matter by Viking, Curiosity, and Perseverance landers/rovers and contribute to the will to drill deeper with Rosalind Franklin rover for geotopes exposed to low radiation doses at a slower rate (Pavlov et al., 2012; Hassler et al., 2014b).

Following MSL, ExoMars and likely Mars 2020 will investigate volcanically/hydrothermally driven siliceous sinter precipitates – induced from crater impacts at Gale and Jezero locations. Scientists discovered these volcanic areas by orbital observations (*e.g.,* at Nili Patera, Arabia Terra, Oxia Planum) (Vago et al., 2017; Goetz et al., 2016) that may have preserved organic matter longer than crater locations explored by MSL (3.6–4.1 Ga). The Curiosity and Perseverance rovers at Gale crater (*Marias Pass*) and Jezero crater (*Alfalfa*), respectively, analyzed diagenetic silica formations. In the Jezero crater rim and Nili Fossae region formed from the Isidis Planitia impactor, the heat released by impact may have driven hydrothermal circulation (*e.g.* (Abramov and Kring, 2005; Osinski et al., 2013),). Those input of nutrients and energy millions of years ago favored proto-cell (and likely evolved life) production following a likely similar pathway to that on primitive Earth and volcanic/hydrothermal areas. The exploration of those extraterrestrial sites for past life traces research encompasses the prediction of desired features and the investigation of conditions and matrices capable of preserving organic matter for millions or even billions of years. To depict such an environment, elemental and molecular keys are needed to interpret *in situ* and return sample analysis via mineralogical, elemental-isotopic, and organic matter observations.

Such features might most probably be explained by abiotic/diagenetic processes, thus, we must analyze the geological context and the bulk elementary and molecular sample to assess organic matter production mechanisms and potential biogenic character of signatures (as the last resort hypothesis, such as isotopic biotic fractionation or various compounds with a strong enantiomeric excess).

Many Martian silica formations have been attributed to diagenetic processes, according to orbiter observations and modeling work (Carr, 1996), consistent with observed phyllosilicate content (Sharma et al., 2023; Squyres et al., 2008; Ruff et al., 2011; Frydenvang et al., 2017). Hydrothermal surface processes (at or below 100 °C) are likely to have occurred billions of years ago, for instance at Gusev crater, Gale crater, Jezero Crater, and Nili Fossae, or likely Oxia planum. Volcanic areas may have favor life cell production and organic matter preservation on Mars time scale (Golombek et al., 2012; Djokic et al., 2017). Therefore, studying Earth volcanic areas with active hydrothermal deposition of silica and/or carbonate minerals is of high interest as potential Mars analogs for the following three reasons. First, to determine the degree of preservation of organic matter in these ancient or modern volcanic locations; second, to understand the organo-mineral interactions relevant to Mars that might preserve these potential traces of life (or biosignatures) and third, to estimate the microbial community that could arise and thrive in these environments to look for precise metabolites (organic compounds used or produced by life) categorized either as bioindicators or biosignatures. Biosignatures can be compounds, physical structures, isotopic or elemental ratios, and characteristics (*e.g.,* enantiomeric excess) linked to biotic processes (Gillen et al., 2023) compared to bioindicators that have the same definition with morphological or composition features explained by abiotic and biotic processes. For instance, Martian methane production might be due to past life production because it is faster than the photolytic destruction in Mars atmosphere and in greater quantity than volcanic trapped gas bubbles' release during successive geological events (Mumma et al., 2009; Webster et al., 2015; Knak Jensen et al., 2014). In addition, if the community finds in the future years $\delta^{12}C$ negative value that clearly discriminate biotic from abiotic inputs we could explain the methane production/preservation with exogenic/atmospheric and surface/-subsurface inputs that create variations in the isotopic $\delta^{12}C$ value like clathrate and some matrix that degrades and reduce organic carbon into methane (Neveu et al., 2018; Prieto-Ballesteros et al., 2006; Gainey and Elwood Madden, 2012).

Martian silica rich deposits may benefit from a combination of geophysical characteristics (*i.e.,* no plate tectonics, slow surface weathering rates, burial by surface regolith, freeze-drying conditions) with a matrix composition protecting organic matter from physical-chemical alterations (*e.g.,* radiations, oxidations, erosions) for thousands of years on the surface and million to billions of years in the subsurface. The preserved organic matter will see a minimal diagenetic degradation in the subsurface environments where Rosalind Franklin rover will drill (Sharma et al., 2023; Carter et al., 2016, 2023). So far, few organic compounds have been identified on Mars at Gale Crater, including chlorine-bearing and sulfur-bearing molecules (Eigenbrode et al., 2018; Williams et al., 2021a; McAdam et al., 2014; Franz et al., 2017), present either as such in the sample, or formed from reaction (chlorination, sulfurization or degradation) occurring in the SAM ovens (Miller et al., 2016; Szopa et al., 2020; Freissinet et al., 2015). Organic compounds once altered by water on Earth or on Mars can either create organo-mineral and organometallic complexes, which might be the case for Mg/Ca/Fe-perchlorates (co-located with organic matter) on Mars (Clark et al., 2021; Archer et al., 2014; Glavin et al., 2013). Organic matter is also oxidized and likely aromatized by radiations and/or GC-MS extraction processes producing PAHs and heteroatom hydrocarbons and aromatics that we observed with SAM and might be explained in crater systems (Eigenbrode et al., 2018; Szopa et al., 2020; Freissinet et al., 2015). At Gale Crater and other explored locations on Mars, no bioindicators have been found yet. The current and future exploration of the sulfate-rich Mount Sharp area by Curiosity, and the sedimentary, and likely the volcanic regions, by Perseverance and ExoMars will be of high interest to the astrobiology community for many reasons, including the potential to detect and identify preserved organo-mineral complexes and heavier organic compounds (Sharma et al., 2023).

Organic matter fingerprints by gas chromatography (high resolution) mass spectrometry (GC-(HR)MS) analysis is often used to trace the source of biomolecules and nutrients, including isotopic analysis on Earth (Mahaffy et al., 2012; Freissinet et al., 2019; Pietrogrande et al., 2013). Indeed, from the mass spectra of different samples, it is often possible to identify the biological source of the organic matter, define the distribution pattern of molecules, and reconstruct metabolic pathways. These metabolites could be preserved in minerals that precipitated at the time of deposition even if cellular material was not directly preserved, making detection via GC-MS within the first centimeters of Martian regolith (or meters with the MOMA instrument onboard ExoMars) possible (Alwmark et al., 2023). Alone these metabolites would not resist to oxidations and radiations, but within silica or mineral matrix it might be preserved for millions of years (Kminek and Bada, 2006; Pavlov et al., 2012; Aubrey et al., 2006; Buch et al., 2022; dos Santos et al., 2016). The combination of elemental and molecular analysis will help strengthen the hypothesis on organic matter preservation conditions and past life traces detection. Thus, we propose in this Mars analog article to combine different laboratory and space-like analysis to study Yellowstone hot springs as a Mars analog. Yellowstone samples helped identify signatures/features likely preserved on Mars if Earth-like life or extent forms of life arose in volcanic/hydrothermal regions. Yellowstone investigations narrow the most appropriate preservation conditions and environments of organic matter in extraterrestrial analog geotopes.

b. Yellowstone's Mars analog bio-geotopes

The Sylvan Spring and Geyser Creek Areas (Gibbon Geyser Basin, Yellowstone National Park, Wyoming, USA) are active hydrothermal areas driven by magmatic heating where siliceous sinter precipitation occurs across a range of temperature and pH values. The hydrothermal fluids are influenced by input from the deep magmatic source, dissolution of volcanic bedrock, and interaction with groundwater to produce water saturated with dissolved silica. Hot springs vary in temperature, pH, and geochemical constituents due in part to subsurface processes, including mixing with groundwater/meteoric water and whether near-surface boiling occurs prior to the fluids reaching the surface. Near-surface boiling drives phase separation (vapor phase and residual liquid phase), and the amount of these phases or minimal phase source fluid feeding a hot spring drive the expressed pH and geochemical environment (Havig et al., 2021). For example, minimal phase separation hot springs (fed by deep hydrothermal source fluids that have interacted with groundwater to some degree) have similar chloride and sulfate concentrations and have circum-neutral to alkaline pH values (from 7 to 14). In hydrothermal areas where near surface boiling drives phase separation, hot springs that are predominantly vapor phase fed will be extremely low in chloride concentration. Additionally, they will be enriched in sulfide when interacting with O_2 from groundwater or the atmosphere that is readily oxidized to sulfuric acid. This oxidation enriches water in sulfates with pH values of 3 or lower, while a predominantly residual liquid phase hot spring will be enriched in chloride and sulfate (increasing concentration due to boiling). Thus, these liquid phases will have pH values at circum-neutral (with neutral pH being approximate 6.3 at boiling). However, dissolved silica concentrations are high in most worldwide hot spring fluids, with discharging fluids precipitating amorphous silica (*e.g.,* Opal SiO_2) as silica becomes supersaturated due to decreasing temperatures and/or evaporation (Navarro-Gonzalez et al., 2006; Campbell et al., 2015). Rapid precipitation of silica onto and around endemic microbial communities can effectively

preserve textural and geochemical signals generated by life (Havig et al., 2021; Campbell et al., 2015; Gangidine et al., 2020; Teece et al., 2022, 2023). However, organic matter can be altered due to overprinting, requiring further study to better constrain the impacts of these effects (Teece et al., 2023; Gonsior et al., 2018).

Temperatures, pHs, and geochemistry parameters impact the composition of the microbial communities present in and around the vent, proximal slopes, distal aprons, and further geothermally influenced environments (Havig et al., 2021; Teece et al., 2022; Finkel et al., 2023). Thus, hot springs can preserve signals from hyperthermophilic to thermophilic chemotrophic communities proximal to vents as well as thermo-to meso-philic phototrophs (*e.g.,* cyanobacteria and other phototrophs (Hamilton et al., 2019; Havig and Hamilton, 2019a)) and heterotrophs that inhabit environments down the outflow channels (*e.g.,* proximal slope, mid-apron), to low temperature distal aprons where eukaryotic organisms are predominant (*e.g.,* algae, plants, and fungi) (Teece et al., 2022).

Here, we report results from samples collected from three hot springs in Yellowstone National Park, USA. Silica sinters were sampled to detect and identify textural and organic matter microbial residues to investigate the potential for preservation of biosignatures in hot springs. Particular targets include organic compounds and organo-mineral complexes that might be involved in processes essential for the living microbial community to thrive, and the influence of pH and temperature on the microbial community (and organic matter composition).

The current study has three main objectives: i) the characterization of geobiological and biochemical signatures directly connected to the presence of life in the three Yellowstone hot springs, ii) the identification of micro-niches for organic compound entombment and sheltering, notably by organo-mineral formations, and iii) the identification of the microbial community in the three different geochemical environments according to the environmental pH and temperatures.

2. Material and methods

a. Sample locations

Samples were collected from three actively siliceous sinter-precipitating hot springs – Dante's Inferno (T 75.9 °C, pH 5.1) in the Sylvan Spring Area, 'Goldilocks' (T 45.4 °C, pH 2.4, Yellowstone Thermal Inventory ID GSSGNN022), and 'Similar Geyser' (T 79.3 °C, pH 8.7, Yellowstone Thermal Inventory ID GGSNN012) in the Geyser Creek Area – located within the Gibbon Geyser Basin, Yellowstone National Park, USA. Sites represent pH values resulting from different hydrothermal inputs – acidic pH/vapor phase dominant, mildly acidic to circum-neutral pH/residual liquid phase dominant, and alkaline/minimal phase separation – with siliceous sinter samples and contextual water samples collected from zones of active silica precipitation from each site (Table 1).

Yellowstone National Park, USA contains a 50 × 80 km diameter 640 Ka volcanic caldera basin formed from hot-spot volcanic activity relating to a hot lower-mantle plume beneath the North American Plate, producing dozens of distinct hydrothermal areas with hot springs exhibiting wide array of temperature, pH, and geochemical characteristics (Hurwitz and Lowenstern, 2014). The Sylvan Springs Area (SSA) in the NW region of the Gibbon Geyser Basin is an approximately 90,000 m^2 hydrothermal region located on hydrothermally altered kame deposits overlying glacial till from the ~21 to 13 Ka Pinedale Glaciation, deposited on Member A of the 640 Ka Lava Creek Tuff (Waldrop and Pierce, 1975). Most of the hot springs occur along a presumed E-W trending fault cutting through the kame deposit, fed by hydrothermal fluids that have undergone near-surface boiling and phase separation (with a detailed description of subsurface processes driving hot spring geochemical expressions in (Havig et al., 2021)). Hot springs in the SSA can be categorized as acidic (pH < 3.5) predominantly vapor-phase fed (*e.g.,* 'Goldilocks'), circum-neutral (pH 5 to 7) predominantly residual liquid phase (*e.g.,* Dante's Inferno), or a mixture of these to end members. The Geyser Creek Area (GCA) in the SE region of the Gibbon Geyser Basin is an approximately 80,000 m^2 hydrothermal region located on Pinedale glacial rubble and till overlying the intersection of Member A of the 640 Ka Lava Creek Tuff (NE), the 208 Ka Paintpot Hill Dome of the Mallard Lake Member Plateau Rhyolite (W), and the 160 Ka Nez Perce Creek Rhyolite Flow of the Central Plateau Member Rhyolite (SE). Similar to SSA, GCA hot springs are predominantly vapor phase, residual liquid phase, or a mixture of the two, but there are also limited occurrences of circum-neutral to alkaline (pH > 6.5) minimal phase separation hot springs (*e.g.,* 'Similar Geyser'). Siliceous sinter samples were collected from the active precipitation zone near the photosynthetic fringe in the outflow (46 °C) just below the primary vent of 'Goldilocks' (a digitate structure, GI Dig), from the active precipitation chemotrophic zone where temperatures had cooled to 25 °C and a nearby abandoned/inactive recent outflow channel of Dante's Inferno (DI Active and DI Old, respectively), and from the active precipitation chemotrophic zone in the outflow channel near the vent (79 °C) of 'Similar Geyser' (a digitate structure, SG Dig).

Table 1
Physical-chemical characteristics of siliceous sinters and associated hydrothermal water.

	'Goldilocks'	Dante's Inferno		'Similar Geyser'
	GI Dig	DI Active	DI Old	SG Dig
Water pH	2.39	6.16	6.16 (estimated)	8.72
Water temperature (°C)	45.70	25.10	25.10 (estimated)	~80
wt% C (= TOC)	0.47	1.00	0.26	0.09
wt% N	0.07	0.07	0.05	0.02
$\delta^{13}C$ (‰, vs. VPDB)	−17.21	−23.78	−21.03	−11.50
$\delta^{15}N$ (‰, vs. Air)	−2.31	−3.68	1.09	6.42
$\delta^{18}O$ (‰, vs. VSMOW)	5.55	10.45	8.33	−1.63
$\delta^{18}O$ (‰, vs. VSMOW) of surface water samples	−14.33 ‰	−9.34 ‰	N.D.	−14.79 ‰
Rhyolite quartz $\delta^{18}O$ (Bindeman and Valley, 2000; Hanson et al., 2018)	4.3 ‰	7.6 ‰	7.6 ‰	N.D.
^{51}V (MR)	0.0004%	0.0008%	0.0004%	0.0004%
^{33}Cs (MR)	0.0001%	0.0030%	0.0030%	0.0383%
^{31}P (MR)	0.0049%	0.0059%	0.0030%	0.0039%
^{75}As (MR)	0.0065%	0.0060%	0.0055%	0.0052%
^{24}Mg (HR)	0.0000%	0.0180%	0.0010%	0.0117%
^{39}K (HR)	0.1679%	1.2882%	0.1460%	0.2487%
^{44}Ca (HR)	0.2566%	0.3383%	0.2370%	0.3434%
^{56}Fe (HR)	0.1816%	0.5790%	0.1730%	0.6686%
^{69}Ga (MR)	0.0002%	0.0018%	0.0003%	0.0160%
^{55}Mn (HR)	0.0040%	0.0064%	0.0053%	0.0053%
^{23}Na (HR)	0.2680%	0.7826%	0.3320%	0.8601%
^{27}Al (HR)	0.3903%	2.5590%	0.3410%	0.6620%
^{32}S (TQ and CHNOS)	1.1750%	7.2727%	0.8667%	0.4500%

N.D.: no data, HR: high resolution, MR: medium resolution from the ICP-MS analyzer. Sulfur was detected thanks to a CHNOS and ICP-MS triple quadrupole analyzers.

b. Sampling procedure

Samples were collected with solvent cleaned (methanol and dichloromethane) and heated (at 500 °C for 8 h in an oven) chisels, spoons, and tweezers. Rock hammers were covered in a piece of heated (at 500 °C) foil before use then removed for sampling. Samples were placed in these clean aluminum foil within sterilized glass jars and stored on ice for transport back to the laboratory. Fresh solvent-washed tools were used for each sample to limit cross-contamination between samples. Samples were stored at −20 °C freezer in laboratory until

analysis. *In situ* analyses have been carried out to measure temperature and pH of hot spring waters/sinters. Hot spring waters have been subsamples for isotopic analysis in laboratory.

In the laboratory, sinters from glass jars were subsampled by breaking off smaller pieces with solvent-washed and flamed tweezers. These subsamples were either powdered for 3 min with a ceramic mortar and pestle that have been solvent-washed (methanol, then hexane, then dichloromethane) and heated (to 500 °C). This grounding step was used to obtain a powdered sample for X-ray diffraction (XRD), inductively coupled plasma mass spectrometry (ICP-MS), isotopy, total carbon/organic carbon/inorganic carbon and total nitrogen contents (TC/TOC/TIC and TN), and gas chromatograph mass spectrometer (GC-MS) analysis. We kept the non-powdered samples for surface analysis: scanning electron microscope (SEM) and Raman. As samples were carefully collected with organically clean tools and techniques in the field, samples were not treated to remove potential natural external contamination before powdering. The MS analyses confirmed the very few (for SG Dig) or absence of contamination for all powdered samples during the sampling and sample preparation for the different analyses. Indeed, helium and solvent GC-MS blanks revealed clean spectra after the analysis of each sample and each replicate with a low background baseline. Moreover, we did not detect fatty acids or other contaminants from human manipulations (*e.g.,* palmitic acid, stearic acid, phthalates, etc.) on negative and positive controls we performed on rock powders simulants without living cells and FAMEs' standard to produce the calibration curve.

Temperature, pH, and conductivity were measured *in situ* using a WTW 330i meter and probe (Xylem Analytics, Weilheim, Germany) and YSI 30 conductivity meter and probe (YSI Inc., Yellow Springs, OH).

Water samples were collected and analyzed as described previously (Havig et al., 2021). In short, water was collected with an acid-washed 140 mL syringe, filtered through a 37 mm, 0.2 μm pore size polyethersulfone syringe filter, and distributed into cleaned sample bottles for anion, cation, dissolved inorganic carbon (DIC), and dissolved organic carbon analysis. Samples were kept on ice (anion, cation, DIC) or frozen (DOC) until analysis. Anion and cation samples were analyzed by the Quantitative Bio-element Imaging Center (QBIC) at Northwestern University via a Thermo Scientific Dionex ICS 5000+ ion chromatography system and a Thermo iCAP 7600 Inductively Coupled Plasma Optical Emission Spectroscopy (ICP-OES), respectively. DIC and DOC samples were analyzed by the Stable Isotope Facility (SIF) at the University of California, Davis via GasBench II system interfaced to a Delta V Plus isotope ratio mass spectrometer (IR-MS) (Thermo Scientific, Bremen, Germany) for DIC and using an O.I. Analytical Model 1030 TOC Analyzer (O.I. Analytical, College Station, TX) for DOC.

c. Imaging and mineralogy of siliceous sinters

The samples were gold coated to better resolute the image and be able to conduct energy dispersive X-ray spectroscopy (EDX) analysis on the four amorphous Opal-A_N samples. SEM images of sinter were collected with a Phenom ProX G5 tabletop environmental SEM. Qualitative analyses were conducted by using a 3 mm spot size, a beam current of 2.25–2.33 nA, and an accelerating voltage of 15 kV under low vacuum conditions consistent with environment SEM operation.

Mineralogy was determined on a 0.5–1 g powdered sample through X-ray diffraction with a PANalytical X-Pert Pro Powder X-Ray Diffractometer (Cu $K\alpha_1$ radiation, $l = 1.540598$ Å, Empyrean Cu LFF (9430,033 7300x) at 45 kV and 40 mA) and patterns were acquired from 5° to 70° 2θ (with a 0.0084° step size for a continuous scan mode). To semi-quantify we introduced two internal standards that are not present in the samples with known mineralogical XRD spectrum (*i.e.,* zincite and corundum at 10 wt%) following the methodology of (Havig and Hamilton, 2019b). However, this semi-quantification was not useful since the abundance in minerals were very low (less than 5 wt% in total) and was primarily composed of quartz.

To characterize the organo-mineral structures and correlation spots on the samples and confirm some XRD mineralogic identification, we first performed Raman analysis on a HORIBA micro-Raman instrument (2–4 μm resolution using a 40× objective, 0.3 D Filter, 200 μm hole) using a 325 nm ultraviolet (UV) laser excitation source slightly different from the deep-UV (248.6 nm) source onboard SHERLOC instrument (Corpolongo et al., 2023). For the sample preparation, we solvent washed (with ethanol) the plastic holder to prepare an Epoxy pellet with arising on one of the surface a piece of sample from the broken pieces (10:1 EpoxySet Resin:EpoxySet Hardener made of bisphenol A and triethylenetetramine, respectively). The analyzed Raman surface was flattened homogeneously with the fewest frictional alterations using sequentially 800, 600, 400, 240, 40, and 1 μm Al_2O_3 sheet (for a final roughness lower than 1 μm).

d. Elementary analysis of siliceous sinters

Elementary analyses were conducted using an Element-2 (Thermo-Finnigan) multi-resolution, single collector, magnetic sector plasma mass spectrometer (ICP-MS). We used 50 mg of sample that was digested using first 5:1 eq. vol/vol HF:HNO_3 ultrapure (Optima) solvents for 8h at 100 °C, then by 6N HCl (after HF evaporation) for 8h at 100 °C (evaporated at the end as well). We then added an aqueous (pure Milli-Q grade water (TOC lower than 3 ppb)) solution made of HNO_3 (5%), Re-Rh (8 ppb internal standard), and HF (150 ppm) for 8h at 100 °C. Finally, we used the later solution to dilute by 2000 the digested mixture. The analyses were made in duplicate and for each analysis, scans were made in six replicates with a medium resolution of 4000 and 5 % of error bars in the results.

For TIC/TOC/TC/TN and isotopic analyses, we used 20–50 mg of samples to get 20 μg of nitrogen and 20–200 μg of carbon range. For the organic matter content, we used three standards called HOS (high organic sediment from Elemental microanalysis), LOS (low organic soil from elemental microanalysis), and atropine (from Costech analytical technologies). The isotopic analyses were conducted in six replicates and normalized according to one geological standard close to our siliceous sinters, namely the HOS standard. It was compared to two organic rich standards usgs 40 and usgs 41 (L-glutamic acids depleted or enriched in ^{12}C and ^{14}N, respectively) before and after the samples at two different concentrations to quantify TC and TN on the wide and unknown content range. TIC analyses were conducted on a Coulometer CM5017 using a phosphoric acid titration of potential carbonates in samples. TC, TN, $^{15}N/^{14}N$, and $^{13}C/^{12}C$ analyses were performed by combustion in a Costech Elemental Analyzer coupled online to a Finnigan-MAT Delta-Plus XL isotope ratio mass spectrometer with a ConFlo III. For ^{18}O, we used Ag cups instead of Sn cups (^{15}N and ^{13}C) and a Thermoconversor analyzer. The values were calibrated to the Vienna Pee Dee Belemnite (VPDB) scale using within-run cellulose standard Sigma Chemical C6413 calibrated against NBSG DIG9 and NBS22 that were included within the runs. TOC and TN were measured on the same instrument.

e. (Pyrolysis, wet-chemistry, and solid phase micro-extraction)-GC-MS material and preparations of siliceous sinters

To perform the organic matter volatilization, we processed the samples using a pyrolysis method at 600 °C or a wet-chemistry untargeted environmental method with dimethylformamide dimethyl acetal (DMF-DMA), tetramethylammonium hydroxide (TMAH), or trimethylsulfonium hydroxide (TMSH). Stainless steel capsules were filled with 5–10 mg sample, 5–10 μL derivatization reagent (DMF-DMA, TMAH or TMSH), and 1 μL of an internal standard ([D8]naphthalene diluted at 10^{-3} mol L^{-1} in dichloromethane – Aldrich, purity >98% and isotopic purity ~ 99 atom % D). This standard was chosen because it is inert to the derivatization and thermal processes, and fully vaporized at 500–600 °C. The capsules were loaded in an EGA/PY-3030D micro-oven pyrolyzer (Frontier Lab). The pyrolyzer was connected to the Split/

SplitLess (SSL) Optic 4 injector (GL Sciences) of a Trace GC Ultra gas chromatograph coupled to an ISQ LT quadrupole mass spectrometer (Thermo Scientific). The injector part was set at 300 °C to avoid a cold trap ahead of the GC column. The electronic impact ionization source energy used was 70 eV. The ions produced were analyzed in the m/z range of 40–500 u. Analyses were performed in full scan mode.

A pyrolysis and derivatization temperature program similar to SAM and MOMA programs were used with a SAM/MOMA-like extracting pyrolyzer device under Martian conditions for this Mars analog study. We performed flash pyrolysis and thermochemolysis at 500 °C and 600 °C. To flush organic compounds into the GC inlet Helium (99,9999% purity, Air Liquide) was used as the carrier gas with a constant flow rate in the column set to 1.2 mL min^{-1}. During the pyrolysis step, the pyrolysates were trapped with at the chromatographic column head using a cryo-focusing set up cooling down a few centimeters of the column head to −180 °C. Once the pyrolysis is done, the cooling is stopped and the column head is quickly heated to the oven temperature. The split flow was 30 mL min^{-1}. The MS ion source was set at 350 °C. The temperature of the transfer line from GC to MS was set to 300 °C.

To achieve the separation of the analytes, a 30 m long capillary column (MXT-5, supplied by Restek) with a 0.25 mm internal diameter and 0.25 mm thick was used. The column was equipped with a 5 m integrated guard column where the cryotrap was installed to pre-concentrate organics before GC-MS analysis. The temperature programming of the column started at 50 °C and increased up to 310 °C at a rate of 5 °C min^{-1}, and was held for 3 min. Blank runs with or without DMF-DMA, TMAH or TMSH (“solvent-blank’’ without sample injection) were performed between each sample analysis to determine and subtract any background level of residual organic matter in the column.

The molecular identification with GC-MS was processed by comparison to the National Institute of Standards and Technology (NIST) reference mass spectra library and using the XCalibur 2.0 software with its peak attribution function. We have been careful to exclude matched molecules with a Reversed Search Index (RSI) and Similarity Index (SI) lower than 700 – corresponding and inverse research corresponding factors comparing our mass spectrum of the GC peak selected and the most similar mass spectrum of the organic molecules from the library. The XCalibur program was also used to interpret the data.

The identification of FAMEs from the analog samples was verified by comparing retention times and mass spectra of a chromatogram obtained from the analysis of a standard mixture of pure FAMEs, alkanes, or PAHs (1000 μg mL^{-1} each component in hexane – Sigma-Aldrich, 99.9% purity).

To quantify the organic recovery and test the reagents’ efficiency for each organic molecule, we measured the peak area of each molecule in the chromatograms and divided it by the peak area of the internal standard (IS, or [D8]naphthalene) using Thermo Scientific XCalibur software. We also performed calibration curves with FAMEs, alkanes, and PAHs standards.

$$A_{organic} \Big/ A_{internal\ standard} = \frac{Areaoftheorganiccompoundpeak}{Areaoftheinternalstandardpeak}$$

On-fiber SPME derivatization headspace extraction was performed loading the derivatizing reagent on DVB/PDMS SPME fiber by exposing the fiber in a 4 mL vial containing 5 μL of PFBCF or 1 g of PFBHA at 30 °C or 50 °C, respectively, for 5 min. After that, the loaded fiber was transferred to another 4 mL vial containing the sample extracted with 0.5 mL of pure Milli-Q grade water for 1 h at 30 °C or 50 °C, respectively. 0.5 g of sodium chloride was added to water extraction to improve the organic compounds volatile.

Gas chromatography analysis was performed with an Agilent 6530 GC with, and Agilent 5973 MS operated in electron impact (EI) mode (70 eV) was equipped with a Zebron ZB-1MS gas chromatography column 30 m × 0.25 mm x 0.25 μm (Phenomenex, USA). The SPME fiber desorption was operated in the GC inlet at 280 °C in a splitless mode for 5 min using Helium (99,9999% purity, Air Liquide) as the carrier gas with a constant flow rate in the column set to 1.2 mL min^{-1}. The GC temperature was programmed as follows: start temperature of 40 °C (held for 2 min) and increase to 300 °C at 10 °C min^{-1} (held for 10 min). The interface GC and MS was set at 310 °C. The temperatures of the ion source and quadrupole were 230 °C and 150 °C, respectively. The mass spectrometer was operated in a mass range of m/z 50 to 500.

3. Results

a. Structural and composition characterizations

i. Imaging analysis

First, we characterized geobiological and biochemical signatures to look for the preservation of organic matter and cells in the three hot springs from acidic to basic pH [2.39; 8.72] range.

SEM-EDX imaging (Fig. 1 and Supplementary Material 1 – SM1) was used to characterize the sample surface, internal structure, and primary elemental composition. First, we visually observed green pigmented biofilms on the surface of Gl Dig and confirmed by SEM visualization of biofilm filaments (Fig. 1 and SM1). We also noted yellow chemotrophic biofilms on the sample at the time of collection due to different pH biotopes. Second, the EDX analysis helped confirm the presence of (bio) geological features, such as pyrite nodules observed as well in previous studies in the same springs (Dante’s Inferno and ‘Goldilocks’) (Loewen and Bindeman, 2016) or filaments (in ‘Goldilocks samples) (SM1). We noted in SEM-EDX imaging the enrichment in iron and sulfur, or in nitrogen, carbon, and phosphorous, to the nodule and biofilm formations, respectively. We noted the preservation of morphological cell signatures in the most acidic samples along with a broader diversity and content range in heteroatoms.

ii. Elementary analysis

We conducted ICP-MS elemental analysis to quantify what we observed in SEM-EDX analysis to confirm hypothesis on the Fe-S amount present locally or uniformly in the matrix, for instance. A low concentration in iron and sulfur would lead as first approach to biotic concentration around the biofilm and biological filaments observed in SEM-EDX. On the opposite, an overall high concentration would most likely lead to an input from the surrounding water that precipitated within collected silica sinters and would remain available for the hypothetical populations observed in SEM-EDX (Table 1 and SM1).

The most abundant elements in the amorphous silica samples, except silicon and oxygen are iron, sulfur, sodium, and aluminum, then calcium and potassium. These results confirm the high abundance of Fe (and S with a triple quadrupole ICP-MS) precipitates observed in SEM-EDX. The quantity of ~0.1–0.6 % on average and for some specific sulfur-rich locations between 1 and 7 % (SM1) might reveal organisms’ species based on sulfur metabolisms (*e.g.,* organisms in DI Active and GI Dig). Previous studies on other alkaline hot springs have reported the enrichment of Mn, Fe, Ga, and S associated with preserved microbial traces or cells as we also report for SG Dig (SM1) (Havig et al., 2021; Gangidine et al., 2020).

iii. Isotopic analysis

In Table 1, we reported the isotopic measurements of three main elements: i) carbon from organic matter to identify enrichment in ^{12}C due to microbial autotrophic (CO_2-fixing) metabolisms (Havig et al., 2011); ii) nitrogen in organic matter to identify potential ^{15}N depletions or enrichments indicative of microbial mediated nitrogen redox reactions; and iii) ^{18}O to track geophysical signature to retrace the geological history of the site and the sample. ^{18}O tracks the temperature variations in the geological layers, and finally $\delta^{18}O$ demonstrates the

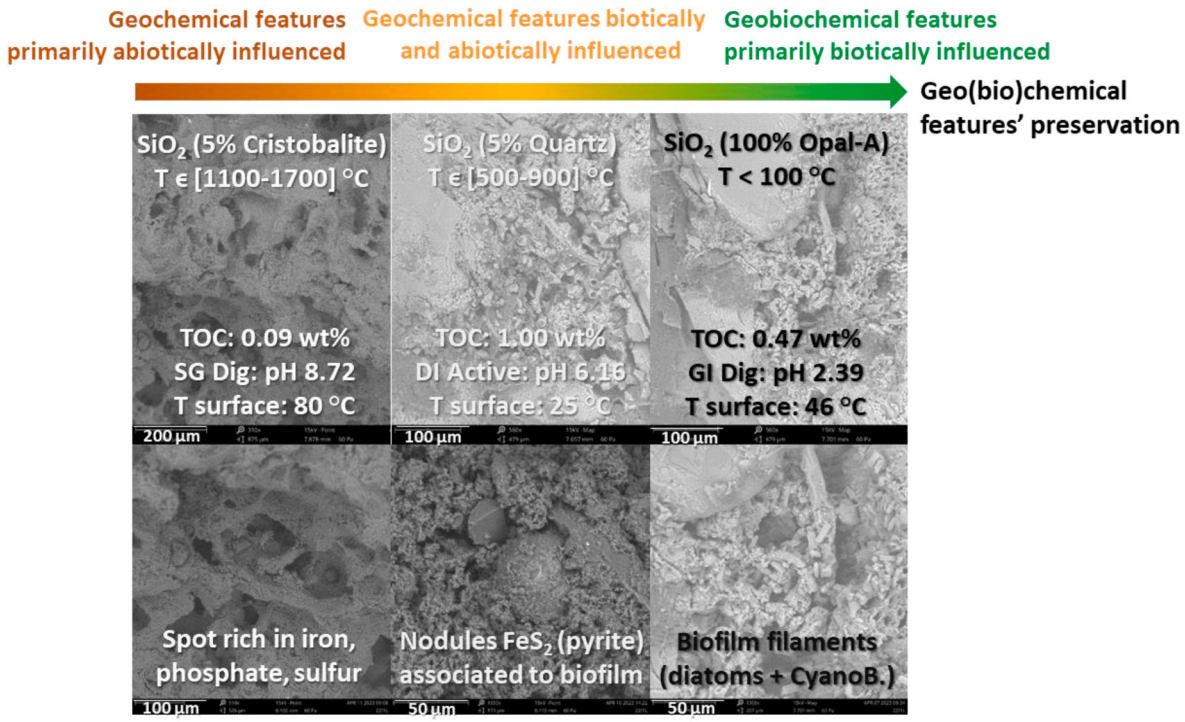

Fig. 1. Physical and elementary results based on SEM-EDX, temperature and pH probes, TOC, and XRD analysis following a pH gradient that might follow a biotic-abiotic geo(bio)chemical feature preservation gradient in samples collected in poly-extreme (SG Dig) to mesophilic (DI Active) environments.

depletion in ^{16}O by oxygenic species due to some photosynthetic organisms (*e.g.,* algae).

The most negative $\delta^{13}C$ and $\delta^{15}N$ values were observed in samples with the lowest surface water temperature, as observed in previous studies with the same $\delta^{13}C$ values (Rull et al., 2022) meaning the most abundant microbial community in cooler spring pools, discriminate ^{13}C from ^{12}C for their metabolism. This result is consistent with the reduced number of organisms that can tolerate temperatures higher than 65 °C (thermophilic and hyperthermophilic extremophiles).

iv. Minerals connected to organic matter and their likely interaction

The overall mineralogy determined by XRD analyses of the four samples were made of an amorphous opal-A_N silica phase that contain 1–5 % of crystalline phase in addition to the 0.1–1 % of organic carbon observed with TOC analyses (Table 1 and Fig. 2). The crystalline phase includes quartz (present in all samples), cristobalite ('Goldilocks'), and pyrite (Dante's Inferno). The relatively older precipitates collected from compacted areas not directly in the outflow of Dante's Inferno (DI Old) contained higher percentage of quartz compared to modern precipitates

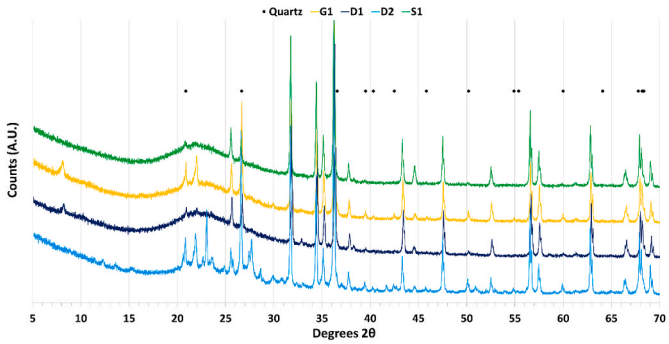

Fig. 2. XRD spectra of the four samples with the two internal standards (zincite and corundum) and the most abundant crystalline form observed (quartz).

from this active hot spring, interpreted as early diagenesis that already occurred compared to fresh silica precipitates at the surface of the hot spring (DI Active). However, no pyrite was detected most likely due to the low wt% in the samples.

The Raman spectroscopy with a UV laser excitation source helped confirm the major minerals and the co-localization of some minerals (*e.g.,* pyrite) with organic matter (SM2). We first noted the difference between the Raman spectrum of the epoxy polymeric matrix without organic matter detected and the locations where the samples arisen with trapped organic matter before interpreting organo-mineral correlations (SM2).

In the Raman analysis (SM2), we observed organic matter likely associated with the degradation of lipids and other metabolites – with the Raman D and G bands due to defect in graphitic structure and C-C bond from sp^2 orbital, respectively, but also a weak bond of C-O-C at 800 cm^{-1}, a weak band characteristic of carboxylic acid dimer at 910-960 cm^{-1}, and likely aromatic rings between 990 and 1050 cm^{-1}, 1365–1450 cm^{-1}, 1450–1505 cm^{-1} within the carboxylic acid, D and G bands. Indeed, they are associated rather than originated from the environment since we observed in GC-MS analyses a low abundance of (a)biotic native PAHs produced in hydrothermal process in low proportion comparing hot spring apron and further precipitates. Specifically, we observed the G-band characteristic of kerogens (1500-1600 cm^{-1}) (SM2). For the samples with and without epoxy (SM2), we observed few peaks at 450-490 cm^{-1}, 550-600 cm^{-1}, and 700-850 cm^{-1}, consistent with the predominantly silica matrix and previous works on similar matrix and environments (Corpolongo et al., 2023; Zeng et al., 1992).

b. Lipidic and metabolomic analysis

Following elemental analysis, we conducted molecular analysis to interpret the microbial community diversity, the organic matter preservation in different environmental conditions, and the efficiency of SAM and MOMA sample processing and analysis to extract and detect biosignatures.

As explained in the materiel and methods, the MS analyses confirmed the very few (for SG Dig less than 10 % of the analytes' quantity) or absence of contamination for all samples during the sampling and sample preparation for the different analyses. Thus, we did not need to prepare the sample by solvent-wash or sterilization at 50 °C for few hours in order to free from human contaminations to get less than 10 % in quantity, especially in palmitic and stearic acids.

For Pyrolysis: 1: Butanal, 3-methyl-; 2: (N-(2-acetamido))-2-aminoethanesulfonic acid; 3: 1H-pyrrole; 4: Toluene; 5: Pyrrolidine, 2-butyl-1-methyl, 6: Furfuraldehyde; 7: 1H-pyrrole, 1-methyl-; 8: 2-furancarboxaldehyde, 5-methyl; 9: Phenol, 10: 1H-pyrrole-2,5-dione; 11: 2,2-dimethyl-4-octenal; 12: 1H-pyrrole-2-carboxaldehyde; 13: Thiophenone; 14: Benzeneacetaldehyde; 15: Phenol, 3-methyl; 16: Undecanol; 17: Levoglucosenone; 18: Succinimide; 19: Benzene, 1-isocyano-2-methyl-; 20: D8-naphthalene (internal standard); 21: Unknown compound; 22: Benzofuran, 2,3-dihydro-; 23: Glucopyranose, 1-thio-, 1-(N-hydroxybenzenepropanimidate); 24: Tridecene; 25: Tridecane; 26: Indolizine; 27: o-tolunitrile, a-cyano-; 28: Benzene, heptyl-; 29: Bicyclopentyl-2,2′-dicarboxaldehyde; 30: Hexadecanol; 31: nonadecane; 32: 1H-indole, 1-methyl-; 33: Carbonimidodithioic acid, methyl-, dimethyl ester; 34: Octadecenal; 35: Heptadecane; Hexathiane; 36: Cetene; 37: Hexadecane; 38: Eicosene; 39: Nonadecene; 40: Phenol, 3-phenoxy; 41: Thiosulfuric acid, S-(2-(cyclopropylamino)-2-iminoethyl) ester; 42: Hexacosene; 43: Sulfurous acid, hexyl octyl ester; 44: Cyclic octaatomic sulfur; 45 to 47: Unknown compounds; 48: Tetracosane; 49: Hexadecanenitrile; 50: Unknown compound; 51: Dipentamethylenethiuram hexasulfide; 52: 2-pentadecylfuran; 53: Unknown compound; 54: Tetratetracontane; 55 to 59: Unknown compound; 60: Carbonic acid, eicosyl vinyl ester; 61 to 66: Unknown compound. The peak 55 that has a significant peak area belongs to a sulfur-bearing compound.

For TMAH: 1: 4-aminopyridine; 2: Methanesulfonic acid, methyl ester; 3: 2,4-dithiapentane; 4: Unknown compound; 5: Dimethyl sulfone; 6: Ethyl methyl sulphone; 7: 2-furancarboxaldehyde, 5-methyl; 8: 1,2,4-trioxolane, 3-phenyl-; 9: Glyceraldehyde, dimethyl ester; 10: Benzene, (methoxymethyl)-; 11: Butanedioic, dimethyl ester; 12: Phenol, 3-methyl; 13: 2,5-pyrrolidinedione, 1-methyl-; 14: Benzoic acid, methyl ester; 15: D8-naphthalene (internal standard); 16: Hepta-2,4-dienoic acid, methyl ester; 17: 1,3-benzenediol, 4-ethyl-; 18 to 22: Unknown compounds; 23: Benzaldehyde, 4-methoxy-; 24: 1H-indole, 1-methyl-; 25: Carbonimidodithioic acid, methyl-, dimethyl ester or 1,3-dithiole-2-thione; 26: Unknown compound; 27: Heptadecane; 28: 1,3-dimethyl-3,4,5,6-tetrahydro-2(1H)-pyrimidinone; 29: Phenol, 3,4-dimethoxy-; 30: Proline, 1-methyl-5-oxo-, methyl ester; 31: 1,2,4-trimethoxybenzene; 32: Unknown compound; 33: 2,3,6-triO-O-methyl-Galactopyranose. 34: Unknown compound; 35: 2,3,4-trimethyllevoglucosan; 36 and 37: Unknown compounds; 38: Nonadecene; 39: 2,4(1H,3H)-pyrimidinedione, 1,3,5-trimethyl-; 40: Unknown compound; 41: 2,4,5,6,7-pentamethoxyheptanoic acid, methyl ester; 42 and 43: Unknown compounds; 44: Pentadecane; 45: Unknown compound; 46: Hexacosene; 47: Dodecanoic acid, methyl ester; 48: Tetracosane; 49: Unknown compound; 50: Hexadecane; 51: Diethyl phthalate; 52: 2-propenoic acid, 3-(4-methoxyphenyl)-, methyl ester; 53: Methyl tetradecanoate; 54: 9H-purin-6-amine, N,N,9-trimethyl-; 55: Tetratetracontane; 56: Unknown compound; 57: Octadecane; 58: Pentadecanoic acid, methyl ester; 59: Pentadecanoic acid, 14-methyl, methyl estet; 60: GlcA-DG, permethylated; 61: Hexadecanoic acid, methyl ester; 62: 5,10-diethoxy-2,3,7,8-tetrahydro-1H,6H-dipyrrolo [1,2-a:1′,2′-d]pyrazine; 63: Eicosane; 64: Heptadecanoic acid, methyl ester; 65: Heneicosane; 66: 9-octadecenoic acid, methyl ester; 67: Stearic acid, methyl ester; 68: Fluoranthene; 69: Methyl 10,15-dimethoxycarbonylhexadecanoate; 70: Methyl 9-cis, 11-trans-octadecadienoate; 71: Docosane; 72: Cyclopropaneoctanoic acid, 2-octyl-, methyl ester; 73: Nonadecanoic acid, methyl ester; 74: 2,4,6(1H,3H,5H)-pyrimidinetrione, 1,5-diethyl-3-methyl-5-phenyl-; 75: Pentacosane; 76: Eicosanoic acid, methyl ester; 77: Methyl 14-methyl-eicosanoate; 78: Octacosane; 79: Methyl 20-methyl-heneicosanoate; 80: Nonacosane; 81: Tricosanoic acid, methyl ester; 82: Heptacosane; 83: Tetracosanoic acid, methyl ester; 84: Unknown compound; 85: Methyl 17-methyl-tetracosanoate; 86: Unknown compound; 87: Hexacosanoic acid, methyl ester; 88 to 91: Unknown compounds; 92: Octacosanoic acid, methyl ester.

In flash pyrolysis, we observed on all three sites numerous products from the hot spring community, especially in alkene (C_1-C_{20}) and heteroatom compounds compared to the wet-chemistry treatments. We observed less alkanes in pyrolysis compared to the TMAH and TMSH analyses on all samples with a ratio of even and odd alkanes above two and above a hundred in quantity (checked based on the retention time of a pure alkanes' standard) of C_{13}-C_{25} in pyrolysis and C_{13}-C_{44} using wet-chemistry. We remarked very few lipids detected by pyrolysis compared to wet-chemistry process. Derivatization process extracted lipids and related acids from C_1 to C_{18}. Goldilocks sample, however, ranged up to C_{28} that might be explained by acidic pH waters where heavier n-fatty acids like octacosanoic acid (boiling point at 430.5 °C) are produced in higher quantity for their acidophilic lipid membrane. On the opposite, we detected benzene, toluene, and fluoranthene for Goldilocks' sample and all pre-treatments. Together with the lipid analysis by TMAH and TMSH, we can reconstruct a part of the microbial community and identify the following families/orders for each sample (Table 2). Overall, the fatty acid-lipidic profile in Fig. 3 and Table 2 is explained by two main communities. The first community demonstrating the major shorter straight and (poly)unsaturated n-alkanes' and n-fatty acids' chain ($<C_{20}$) with an even number of carbon atoms (with in addition the cyanobacterial C_{17}) are associated to eukaryotic and bacterial microbial inputs, whereas longer chains with an odd number of carbons are allocated to higher plants located in the coast of hot-springs only (Harwood, 2012; Gago et al., 2011).

i Solid phase micro-extraction GC-MS analysis

We identified numerous compounds using the SPME fiber method (Table 3 and Fig. 4) that revealed complementary identifications to pyrolysis and thermochemolysis GC-MS analyses, especially with the detection of light aldehydes, amines, ketones, carboxylic acids, and PAHs. For the latter, we identified toluene that might be a by-product of pigment lipids by diagenetic reactions. Indeed, organic matter alteration after disassociation of lipids from cell membranes by bio-chemical processes including hydrolysis, redox, (de)sulfurization, for instance on polyene isoprenoids (Finkel et al., 2023). This hypothesis might be strengthening with the other pigment by-products identified. Regarding aldehydes and ketones, the origin might be from fermentation and oxidant-reduction energetic thermophilic processes (Zeikus et al., 1981; Cady and Farmer). These compounds identified on modern, but also on ancient silica sinters demonstrate the hypothesis that cells entombed by silica precipitation help preserve physical structure and cellular organic matter (Jahnke et al., 2001) on Earth and extrapolated to other planetary systems like Mars. Therefore, based on the overall lipidomics (and metabolomics) work, we identified several bioindicators and primarily gnostic biosignatures within the geobiological, geochemical, and biochemical studies (Table 2).

4. Discussion

The study was focused on Yellowstone National Park hot springs' systems analog to past active volcanic areas or induced hydrothermal systems in Martian crater regions with the aim to depict and differentiate abiotic to biotic then agnostic to gnostic signatures of past or present life. The samples from Dante's Inferno and 'Similar Geyser' were collected from chemotrophic zones of their respective outflows with numerous nutrients bioavailable within a neutral or basic pH (*e.g.*, phosphate, arsenate, and sulfate). Indeed, organisms are drawing their energy from mineral substrates with a renewable source of S, P, Fe, K, Na, Mg, Ca, V, Mn, Co, Ni, Cu, Zn, Mo thanks to the active hot spring outflows. However, in SEM-EDX, we did not observe sheltered living/

Table 2
Selection of interesting gnostic biosignatures (and bioindicators for the light organic compounds below $C_{12\text{-}16}$) or their derivatives (due to biological or chemical transformations) cross-link with literature and the huge effort furnished in previous studies in Yellowstone hot spring systems. These biomolecules might be interesting target to look for during future Mars analysis specific to certain class of metabolites in function of the endemic or extremophilic populations towards the different GC-MS pre-treatments.

Class of metabolites	Actinomycetes (Kumari et al., 2013)	Algae (Hewelt-Belka et al., 2020)	Cyanobacteria (Passos et al., 2023; Carruthers and Lee, 2021)	Metabionta	Thermoacidophiles archaea and acidophilic/thermophilic bacteria (Chatzivasileiou et al., 2019; Koga and Morii, 2005; Koga, 2012; Tomečková et al., 2020)	Euglenophyta (Vinçon-Laugier et al., 2017)	Alkalinophile archaea (Chatzivasileiou et al., 2019; Koga and Morii, 2005)	Sulfate-reducing bacteria (Lamed and Zeikus, 1981)	GC-MS pre-treatment
Linear/saturated fatty acid (FA)	From palmitic acid to arachidic acid (C_{16} - C_{20})	From palmitic acid to melissic acid (C_{16} - C_{30})	From palmitic acid to arachidic acid (C_6 - C_{24})	From palmitic acid to melissic acid (C_{16} - C_{30})	From palmitic acid to melissic acid (C_{16} - C_{30})	From palmitic acid to arachidic acid (C_{16} – C_{18})	From palmitic acid to arachidic acid (C_{16} - C_{20})	From palmitic acid to arachidic acid (C_{18} - C_{20} higher abundance than C_{16} -C_{17})	TMAH TMSH DMF-DMA
Mono-unsaturated fatty acid (MUFA)	N.D.	From 6-heptenoic acid to 11-eicosenoic acid (C_7 - C_{20})	From 9-tetradecenoic acid to 9-octadecenoic acid (C_{14} - C_{18})	From 9-tetradecenoic acid to 9-octadecenoic acid (C_{14} - C_{18})	Vaccenic acid (18:1ω-7) from bacterial lipids	Palmitoleic acid and oleic acid (16:1 and 18:1ω-9)	N.D.	Vaccenic acid and oleic acid (18:1ω-7, 18: 1ω-9)	TMAH TMSH
Poly-unsaturated fatty acid PUFA	N.D.	8,11-octadecadienoic acid and α-linolenic acid (C_{18} from fresh water algae)	9,12-octadecadienoic acid (18:2) and α-linolenic acid (18:3ω-3)	9,12-octadecadienoic acid (18:2) and α-linolenic acid (18:3ω-3)	9,12-octadecadienoic acid that might be from archaeal lipids	α-linolenic acid (18:3ω-3)	N.D.	N.D.	TMAH TMSH
Archaeol	/	/	/	/	Glycerol and tridecanoic acid, 4,8,12-trimethyl- (that might come from for instance diphytanylglycerol) from archaeal lipids	/	Glycerol and tridecanoic acid, 4,8,12-trimethyl- (that might come from for instance diphytanylglycerol)	/	TMSH
Glycerol dialkyl glycerol tetraether (GDGT)	Glycerol	/	Glycerol, galactose that might come from MGDGs and DGDGs.	/	Glycerol, isoprenol, isopentol, mevalonate	Glycerol, galactose that might come from MGDGs and DGDGs.	Glycerol, isoprenol, isopentol, mevalonate	Glycerol, isoprenol, isopentol, mevalonate (only gram-positive metabolites detected)	TMAH TMSH
Diether	/	/	/	/	Octanoic acid, methoxy-, 8-dodecenoic acid, methoxy-, hexadecanoic acid, methoxy-	/	Octanoic acid, methoxy-, 8-dodecenoic acid, methoxy-, hexadecanoic acid, methoxy-	Octanoic acid, methoxy-, 8-dodecenoic acid, methoxy-, hexadecanoic acid, methoxy-	TMAH TMSH
Hopanoid	N.D.	N.D.	N.D.	N.D.	N.D.	N.D.	N.D.	N.D.	/
Alkanol	N.D.	1-dodecanol, 3,7,11-trimethyl-	N.D.	1-dodecanol, 3,7,11-trimethyl-	N.D.	1-dodecanol, 3,7,11-trimethyl-	D.D.	N.D.	TMAH TMSH
Sterol and poly aromatic hydrocarbon (PAH)	cyclopentanophénantrènique	Furan, 2-heptyl, p-cresol, 1H-indole, isoquinoline	N.D.	Furan, 2-heptyl, p-cresol, 1H-indole, isoquinoline	cyclopentanophénantrènique	N.D.	cyclopentanophénantrènique	cyclopentanophénantrènique	Pyrolysis TMAH TMSH
Glycolipid	Galactoseptanoside, Glucopyranoside, and decycled: *(e.g.,* 2,4,5,6,7-pentamethoxyheptanoic acid) with linear lipids identified.	Galactoseptanoside, glycerol	N.D.	Galactoseptanoside, glycerol	N.D.	Galactoseptanoside, glycerol	N.D.	N.D.	TMAH TMSH

(*continued on next page*)

Table 2 (*continued*)

Class of metabolites	Actinomycetes (Kumari et al., 2013)	Algae (Hewelt-Belka et al., 2020)	Cyanobacteria (Passos et al., 2023; Carruthers and Lee, 2021)	Metabionta	Thermoacidophiles archaea and acidophilic/thermophilic bacteria (Chatzivasileiou et al., 2019; Koga and Morii, 2005; Koga, 2012; Tomeckova et al., 2020)	Euglenophyta (Vinçon-Laugier et al., 2017)	Alkalinophile archaea (Chatzivasileiou et al., 2019; Koga and Morii, 2005)	Sulfate-reducing bacteria (Lamed and Zeikus, 1981)	GC-MS pre-treatment
Peptidoglycan	Glucosamine and few amino acids (*e.g.*, norvaline)	/	Glucosamine and few amino acids (*e.g.*, norvaline)	Glucosamine and few amino acids (*e.g.*, norvaline)	N.D.	Glucosamine and few amino acids (*e.g.*, norvaline)	N.D.	N.D.	TMAH TMSH
Other lipidic compounds (and derivatives)	Mycolic acids (*e.g.*, Octanoic acid, 8-hydroxy-, carynomycolic acid)	Betaine that might be connected to the saturated FA, cinnamic acid, terephthalic acid	/	Betaine that might be connected to the saturated FA, cinnamic acid, terephthalic acid	16-methylhexadecanoic acid, 15,16-dimethyltriacontan-dioic acid from bacterial lipids and Benzenepropanoic acid, 4-methoxy	/	N.D. (phospholipids)	8-methylnonanoic acid, 16-methylhexadecanoic acid, 15,16-dimethyltriacontan-dioic acid	TMAH TMSH
Sugar and derivative	Glucose, glycerol	Glucose, glycerol	Glucose, glycerol	Glucose, glycerol	N.D.	Glucose, glycerol	N.D.	Glucose, glycerol	TMAH TMSH

N.D.: Not detected (other than compounds put in other box from the same class of organisms).

fossilized cells or C, N, and P traces from the desiccated biomass for Gl Dig and very few for DI Active and DI Old compared to SG Dig. The observation of pyrite nodules led to the hypothesis that they were globules of elemental sulfur trapped in silica and subsequently consumed by organisms in acidic environment with pyrite precipitation replacement (Loewen and Bindeman, 2016). The correlation between imaging and spectroscopic analysis helped constrain the influence of pH and temperature on the potential preservation of siliceous sinters. Based on these surface analyses, pH seemed to be the main driver of the present microbial community diversity and the resultant silica that precipitated. However, temperature was most likely the primary driver for organic matter and microbial abundance in these systems similarly to other hot springs' systems. In addition, from SEM analysis, we noticed that silica precipitates at several millimeter scales for alkaline pH or at the free ion state at acidic pH with nodules or other crystalline or amorphic phase at 100 μm to few mm scale related to water temperatures. In all samples, the EDX analyzer detected carbon- and sulfur-rich patches where organic matter was correlated to the presence of traces of life observed in SEM (filaments, globules, EPS matrix in SM1). These results provide a valuable input on the preserved active microbial community being currently in the early diagenesis process of these hot springs (Teece et al., 2023).

Some geological features (*e.g.,* pyrite nodules, silica precipitate preserving biological textures) may represent bioindicators – forming as a result of active or passive biological processes – and not biosignatures due to potential abiotic processes that might produce features with similar shape and composition, making their detection in Martian samples ambiguous. However, isotopic analyses (coupled to molecular mass spectrometry techniques) may provide stronger determination of biological provenance because living organisms fractionate elements in favor of their lighter isotopes to save energy during the transport and the metabolization of nutrients. Isotopic fractionation thus represents an agnostic bioindicator or biosignature since only living organisms produce strong fractionations in favor of light elements (Geilert et al., 2015b; Holloway et al., 2011; Thomazo et al., 2009; Vogel et al., 2015). These signatures might also be important for prebiotic chemistry because they are the locations of potential autocatalytic and organic chemistry reactions that might lead to primitive cells (Rimola et al., 2019). Other signatures clearly indicate biogenicity, such as preserved cellular structures/textures and enrichment of co-located C, N, S, and P (Fig. 1 and SM1). While on Earth, these first order discriminations are often based on visual and elementary analyses, current spaceflight missions are not equipped with the capability to image and analyze on micro-to nano-meter scales. Therefore, we must correlate these observations with complementary spectroscopic and mass spectrometry analysis to classify spectral signatures as organic molecules or nutrients essential to life, bioindicators, or biosignatures. This classification would help demonstrating the biogenicity of an analog or extraterrestrial sample. SEM-EDX analyses revealed physical evidence of microbial processes with the oxidation of elemental sulfur spheres coated with extracellular polymeric substances (EPS) biofilms. The biomass clearly noted as filaments and confirmed by a rich organic content in localized EDX and Raman analysis with smaller spheres irregularly shaped due to localized oxidations. The microbial community in acidic environments mediated Fe-S mineral precipitation (and confirmed with GC-MS analyses the presence of pyrite and/or organic matter), consistent with previous work (Loewen and Bindeman, 2016).

Several chemical elements were detected in high abundance for all samples relative to Fe and S (*i.e.,* Na, Ca, K, Mg especially for DI Active) and additional elements co-localized to organic matter (*i.e.,* P, Cs, As especially in SG Dig), according to SEM-EDX and Raman analysis. For Na, Ca, K, Mg, Mn, and V, we hypothesize the presence of minerals in low abundance within the silica matrix (below 5 wt%), *i.e.,* halite, vanalite, corvusite, fritzscheite, rollandite, and hyalophane. Some of them were observed in previous works in Yellowstone hot springs and likely correlated to microbial communities (Havig et al., 2021). The

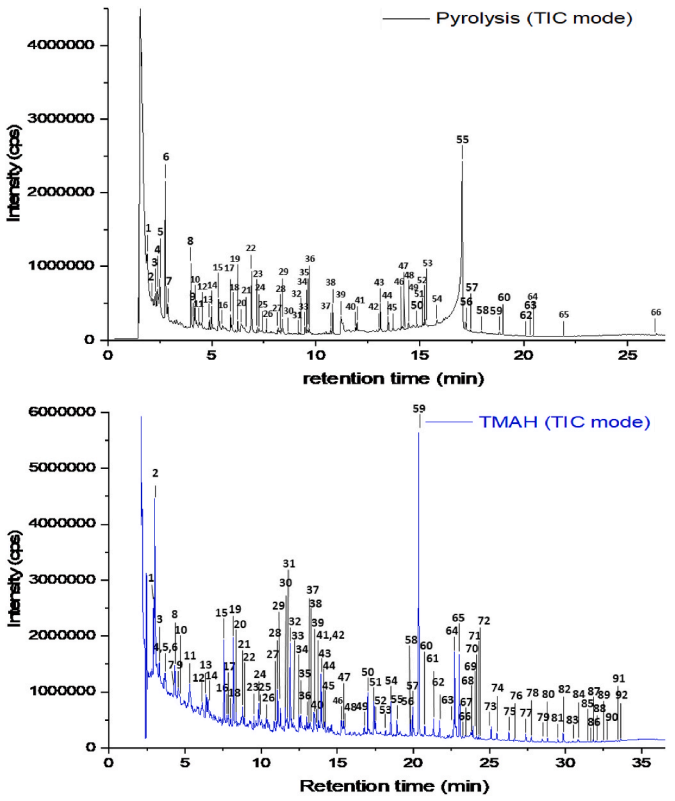

Fig. 3. Total Ion Chromatograms of TMAH and pyrolysis pre-treatments on GI Dig (modern "Goldilocks" – Sylvan spring siliceous sinter) where we identified the following organics (different from the solvent by-products) with few dozens more compounds observed selecting 43, 57, and 143 u).

microbial life assimilates elements for their metabolism (*i.e.,* Mg, V, Mn, Fe, Co, Ni, Cu, Zn, Mo) and releases organic compounds (compatible osmolites and EPS matrix) to agglomerate soil particles and minerals (non-essential biological elements, *i.e.,* Si, Li, Al, Ga, As) to protect themselves from environmental stress (Bundschuh and Maity, 2015; Oremland and Stolz, 2003). These hypotheses have been confirmed by analyzing surrounding rhyolites enriched in the same elements without biofilms in previous studies and other hot spring locations (Havig et al., 2021; Loewen and Bindeman, 2016; Rull et al., 2022). These elements might be helpful to produce organo-mineral complexes and thus help precipitate organic matter on the surface (Jones, 2021). This phenomenon is essential for organic matter and cell preservation over a long geologic time scale in these volcanic systems on Earth and likely Mars. Indeed, the study of organo-mineral complexes might provide a clue to discover (geobiological or biochemical) biosignatures or bioindicators if we first detect a patch of sulfates or pyrite, for instance, and second if we detect organic matter co-located with these minerals on Mars.

However, the presence of sulfates and pyrite has never clearly given an answer to the preservation of organic matter over million to billions of years even if it remains a strong hypothesis based on carbon-sulfur chemistry (Eigenbrode et al., 2018). Thus, geospatial chemical analysis, such as a Raman mapping of organic matter and minerals on a sample might help localize organo-minerals complexes and biosignatures on Mars. In this study, the Raman mapping (SM2) co-located quartz, opal A, and organic matter. However, we did not quantify several % of pyrite or other minerals that may help preserve organic matter, except silica. The bulk analysis in XRD or the surface analysis of Raman did not succeed to identify with certainty pyrite, however, small nodules and fractions of Fe-S minerals have been detected in SEM-EDX in located places of DI Active and GI Dig. This lack of detection is explained by the low wt% of these minerals in the samples and the local

Table 3
List of volatile organic compounds detected after evaporation at 50 °C for 1h on the fiber where PFBHA or PFBCF derivatization could occur to be observed in GC-MS.

Compound name	PFBHA	PFBCF
Toluene	x	x
Pentanal, 3-methyl-		x
Formaldehyde[a]	x	x
Hydroxylamine[a]	x	x
Acetaldehyde[a]	x	x
Hexanoic acid, 2-ethyl-		x
Acetone[a]	x	x
Benzoic acid		x
Carbonic acid[a]		x
2-sec-butylcyclohexanone		x
Propionaldehyde[a]	x	
Octanoic acid	x	
Isobutanal[a]	x	
Butyraldehyde[a]	x	
Nonanoic acid	x	x
1,3-dihydropropanone[a]		x
Butanal, 2-methyl[a]	x	
Pentanal[a]	x	
2,4,4-trimethyl-3-(3-methylbutyl)cyclohex-2-enone	x	
Unknown compound	x	x
Decanoic acid	x	x
Acetic acid[a]		x
3-methylpentanal[a]	x	
Hexanal[a]	x	
2,5-cyclohexadiene-1,4-dione, 2,6-bis(1,1-dimethylethyl)-	x	
Heptanal[a]	x	
Dodecanoic acid	x	
Diethyl phthalate	x	
7,9-di-tert-butyl-1-oxaspiro(4,5)deca-6,9-diene-2,8-dione		x
Octanal[a]	x	
Benzaldehyde[a]	x	
Crotonaldehyde[a]	x	
Phenylacetaldehyde[a]	x	
Nonanal[a]	x	
Hexathiane	x	
Phthalic acid	x	
Glycoldial[a]	x	
Diglycolic acid[a]	x	x
Decanal[a]	x	
1,2-benzenedicarboxilic acid, bis(2-methylpropyl) ester	x	
Ethanone, 2,2-dimethoxy-1,2-diphenyl	x	
7,9-di-tert-butyl-1-oxaspiro(4,5)deca-6,9-diene-2,8-dione	x	
Unknown compound	x	
Unknown compound	x	
Dibutyl phthalate	x	x
Hexadecanoic acid	x	
2-methyl-2-pentenal[a]	x	
Cyclic octaatomic sulfur	x	
Glutaraldehyde[a]	x	
Benzyl butyl phthalate	x	x

[a] derivatized compounds by PFBHA/PFBCF.

precipitation at the negligible 10–50 μm scale compared to the centrimetric scale of the sample, or the few millimeters resolution in Raman. The amorphous silica, and in minor ways the Fe-S crystalline forms producing phyllosilicate sheets and spherical capsules, respectively, helped preserve relatively small amounts (0.1–0.26 wt% of the least preservation site SG Dig and most ancient site DI Old) of organic matter and cells in active Yellowstone hot springs.

Concerning the elements associated with organic matter in our samples, we detected phosphorus, which is essential for the energetic metabolism of all microbial life on Earth, and we also detected relatively high concentrations of As and Cs. These metals are associated with organic matter in geothermal systems and contaminated soils due to mining or industrial factories (Bundschuh and Maity, 2015; Oremland and Stolz, 2003). As and Cs are metabolized by some extremophile organisms (Oremland and Stolz, 2003; Darma et al., 2022; Gihring and Banfield, 2001; Visscher et al., 2020; Sforna et al., 2014). The high percentage in Cs, especially in alkaline silica sinters (SG Dig), is relevant

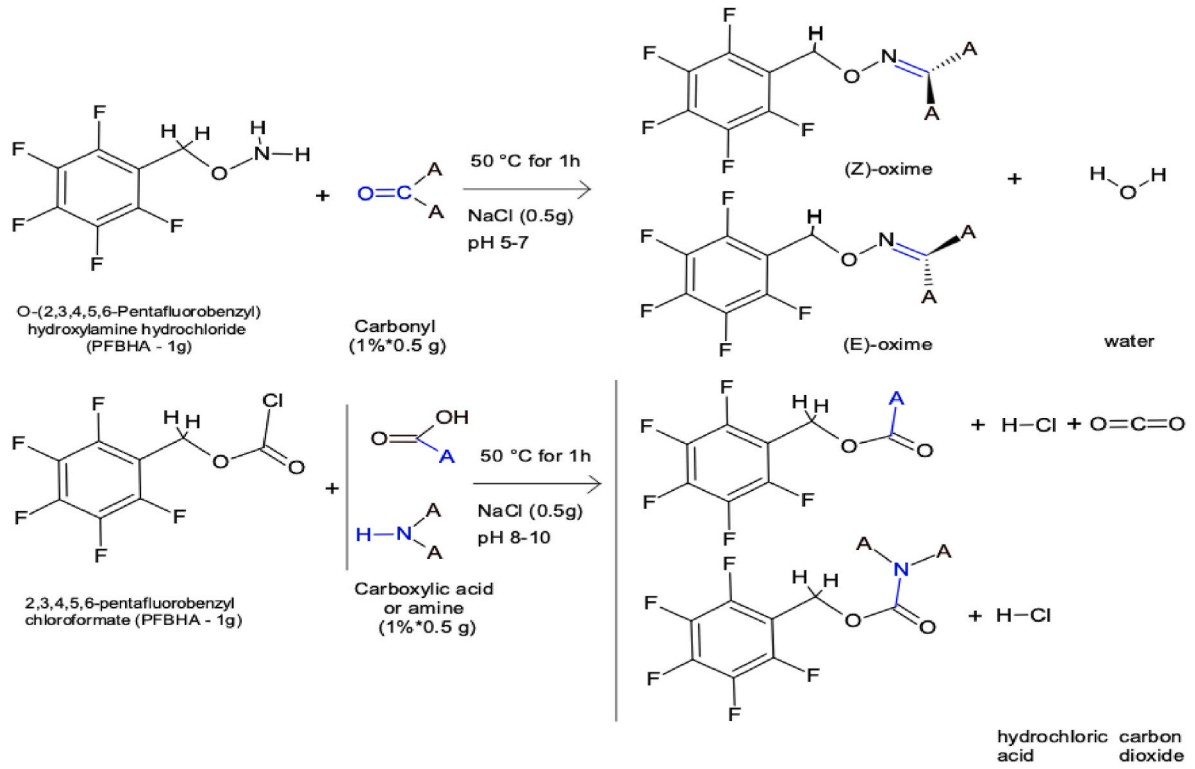

Fig. 4. SPME PFBHA and PFBCF reactions and GC-MS analysis results with the list of compounds identified and specified for the one derivatized.

for our research because on Earth, as on Mars, Cs is generally present in soils at around a few ppb to ppm (Jones, 2021), except when concentrated by a volcanic event and/or by life (associated to organic matter as remarked in SEM-EDX). The relationship between As and life is explained by biotic processes that use these metals for oxidative-reductant reactions for electron exchange in the energetic or secondary metabolisms. The concentrations of As did not show a particular trend in its enrichment relative to pH compared to Cs. Arsenic behaves like phosphorus as oxy-anions, however, As is toxic for microbial life, as opposed to P, which is essential for energetic metabolisms. Microorganisms adapted to As-rich environments can either reduce and precipitate the cation or methylate arsenate anions that volatilize (Gihring and Banfield, 2001). In the three YNP hot-springs investigated here, the amount of As ranged in the same order of magnitude than P, demonstrating that As is reduced and precipitates as a cation, rather than being methylated, because As would have been volatilized and escaped from the silica sinters (Havig et al., 2021).

If on Mars, or other planetary systems, we observe i) a few percentages of these two elements co-located with organic matter and ii) note the detection of As precipitates due to pH that is influenced by life and in a minor way by geological events, which are rare on Mars compared to Earth in volcanic areas, we might hypothesize that life may have arisen on the explored site. This primitive life might have used Cs and P for their metabolisms while they precipitated As in order to access P (or PO_4^{3-}). The validation of those hypotheses on Mars might be easier if we find a correlation between organic matter and As/Cs concentrations, or if As and Cs are concentrated in restrictive volcanic areas compared to surrounding volcanic soils. This correlation would work as bioindicator, and links with other elements like the high concentration of pyrite or high molecular weight organic compounds (above C_{16}), for instance, would lead to a biosignature.

The exploration for hot spring deposits in volcanic systems or from large impact craters on Mars should be a critical analysis and sampling goal for rover missions due to past traces of sustainable water and energy for organic matter to react. The current study and the will to detect these inorganic and organic markers suggest that the instrumentation on board current and future rovers should be ideally suited for detection of geochemical and textural evidence of life (*i.e.,* detection of the biologically important elements C, N, P as well as trace elements such as Mn, Co, and Ni; identification of relevant mineralogy such as amorphous silica, opal, iron-sulfides, and arsenic; and quantitative identification of organic matter).

Finally, elementary analysis revealed macroscopically and then microscopically photosynthetic populations on the shelf further from the hot waters, which correlate with the depletion in ^{16}O (SG Dig). Compared to other hot spring fluids, the investigated biotopes were enriched in ^{16}O (DI Active and Old), which means these samples had a lower biomass than silica sinters. The enrichment in ^{16}O in the acidic silica sinters (Gl Dig, DI Active, DI Old) compared to alkaline sinter (SG Dig) is explained by the tradeoff between: i) the fractionation (depletion in ^{16}O) in the fluvial precipitation for low surface temperature in silica sinters; ii) the enrichment in ^{16}O from rhyolite signals and may be contributed to the sinters by input from ground volcanic rocks; and iii) in a minor role due to an active microbial life in acidic hot springs. Indeed, despite the modern silica sinters collected, we noted a difference with a^{16}O enrichment in silica sinters compared to surrounding waters used to precipitate silica (Table 1). Thus, we might hypothesize that microbial life plays a role in the release of oxygen in the precipitation with an input of ^{16}O, balancing the depletion of ^{16}O from spring waters (Havig et al., 2011), which might lead to another bioindicator marker. Microbial life cannot produce some essential metabolites like some amino acids or sugars, therefore, they need to absorb it from the soil and water to operate their metabolism. This metabolic processes favor the integration of lighter C,N,O-bearing compounds and lighter elements within these inorganic and organic cells' compounds.

The only agnostic biosignature in our analysis is represented by a negative isotopic value for carbon. The lowest $\delta^{13}C$ value at −23.78 ‰ (compared to −11.50 ‰) likely reveals the activity of the photosynthetic biofilms in DI Active (and GI Dig) coolest hot springs. The (hyper) thermophiles do not use the reductive pentose phosphate cycle (PEP) to

fix carbon but the reductive tricarboxylic acid cycle (TCA) that fractionates ^{13}C differently: from −5 to −10‰ for TCA cycle and −17 to −27.5 ‰ for PEP cycle. However, these specific values cannot be by themselves biosignatures for a specific classes of organisms (phototrophs with PEP cycle and chemotrophic with TCA cycle) because some chemotrophic organisms use instead of TCA the acetyl coenzyme A pathway (ACP) where the ^{13}C fractionation range from −5 to −28‰ (Rull et al., 2022; Schuler et al., 2017). Despite the overlap of $\delta^{13}C$ values, a negative value in $\delta^{13}C$ remains an agnostic biosignature because no geological-physical-chemical abiotic process allows such a fractionation in $\delta^{13}C$.

$\delta^{15}N$ values in DI Active and GI Dig are close to zero, which corresponds to the isotopic composition of the atmospheric N_2, demonstrating a strong input of nitrogen from aeolian deposition (and inorganic solutes like nitrates). Therefore, nitrogen is the limiting factor in silica sinters' biofilms with limited concentrations in nitrogen found in SEM-EDX and elementary TN analyses without detection of nitrate in the mineralogical and elementary analyses. This limiting nitrogen is mostly observed in SG Dig with a strong positive value (Rull et al., 2022; Brabandere et al., 2007).

The TOC analysis, $\delta^{13}C$ values, and $\delta^{15}N$ values together would strengthen the discovery of past traces of life or prebiotic chemistry on the Early-Mars surface, if they present a strong depletion in heavy elements with a high concentration in TOC, as we observed in the modern Dante's Inferno site. Indeed, if we compare DI Active with the older layers DI Old collected at Dante's Inferno or SG Dig (at Similar Geyser) the higher temperatures favor different communities with different metabolisms that is presented in this untargeted environmental metabolomics study. Temperatures above 50–70 °C decrease the preservation of organic compounds especially in alkaline soils (with or without a high abundance of oxidants, *e.g.,* perchlorates, sulfates).

In the literature, scientists revealed that biosignatures would most probably be preserved in alkaline and temperatures below 70 °C (Williams et al., 2019, 2021a; Teece et al., 2022, 2023; Reinhardt et al., 2020). These conclusions based on temperature are consistent with the present study where the least organic matter preservation is in the hottest hot spring (above 70 °C all year long). However, the highest organic content and microbial life biosignatures and bioindicators preservation were within the acidic hot springs (*i.e.,* GI Dig and DI Active sinters). Therefore, temperature seems to pressure the most organic matter preservation. pH seems to drive in a minor way microbial life and organic preservation in volcanic and hydrothermal systems, but still significantly with an order of magnitude between acidic and circum-neutral or alkaline hot springs. Concerning geobiological signatures, the acidic pH seems to favor organic compounds' and/or cells' preservation at YNP on the opposite of non-volcanic areas where alkaline environments seem to favor the preservation in silica sinters (Williams et al., 2019). Alkaline environments preserve biosignatures longer than acidic ones in different Earth environments due to the co-precipitation of organic matter and cells with minerals and salts. The latter may protect organic matter from oxidation, erosion, and radiations. However, in hot springs and volcanic geotopes, if the temperature is above 50–70 °C, the co-precipitation might be either too slow before organic matter degradation or does not allow the long-term preservation with a constant water alteration at high temperatures (above 70 °C). Therefore, alkaline geotopes seems to be the best location to investigate on Mars, especially for silica precipitates, clays, or sediments, except for volcanic/hydrothermal-driven environments where the acidic and sulfur rich regions would be most hopeful for organic matter and biosignatures detection on the first radiated and oxidized centimeters or meters, according to Yellowstone and Mars SHERLOC and SAM analysis.

Raman analyses demonstrated that UV laser source help detect organic compounds if well preserved. SHERLOC instrument uses deep-UV laser source, compared to the UV laser source used in this work, which allows for a finer detection of organic matter at the microscale. The sampling process, Raman analysis methodology, and laser sources used on Yellowstone and Mars samples helped detect from 10 to 100 ppm to % of organic matter. However, none of the results highlight clearly the presence of biosignatures. Laboratory Raman revealed the presence of bioindicators (likely connected to gnostic biosignatures) and confirmed by GC-MS. Indeed, together with SEM-EDX and ICP-MS, we may suggest the presence of life in the sample with concomitance of organic matter elements (C, N, S, and P) with metabolized elements (Mg, V, Mn, Fe) and non-essential biological elements pre-concentrated by organisms (Al, Ga, As, Cs) due to biotic concentration processes. Therefore, we need complementary analysis to confirm the hypothesis of co-precipitation between organics and minerals or mineralization of elements induced by certain classes of organisms through a molecular analysis (GC-MS) to depict the metabolites used and track back the classes of organisms that are present (in support of previous genomic analysis).

To ensure the microbial signal detection in a natural sample and quantify biosignatures that were associated and/or protected within the siliceous sinter samples, we conducted lipidomic and untargeted environmental metabolomics analyses. We compared these data with previous studies investigating Yellowstone hot springs and microbial community composition by DNA/RNA sequencing. Previous analyses of samples from Dante's Inferno via 16S rRNA-sequencing confirmed a rich chemolithotroph community based on sulfur and iron metabolisms (Havig et al., 2021). The authors of that study also assumed that the S^0-oxidizing bacteria may be associated with generation of EPS matrix with a dense biofilm entombed and fossilized in these sulfur spheres during the oxidation process. Members of the microbial community were associated with iron (Fe^{III}) reducing bacteria and archaea including *Hydrogenothermales, Desulfurococcales*, *Thermoproteales*. In addition to chemolithotroph populations, photoautotrophs are present in the 'Goldilocks' outflow (where the water temperature is below 72 °C and sulfide concentrations do not inhibit phototrophy), including cyanobacteria and algae (Havig and Hamilton, 2019a). These photosynthetic organisms produce an abundant amount of organic matter for their metabolic input, leading to higher concentrations of TOC in the modern precipitate samples compared to other sites (*e.g.,* DI Old) or hot springs with a lower biomass (*e.g.,* SG Dig chemotrophic zone).

The detection in GC-MS (pyrolysis mode) of alkene (C_1-C_{20}) and heteroatom compounds compared to the wet-chemistry treatments revealed, for most of them, the origin of these organics. Indeed, these compounds are metabolite by-products degraded at 600 °C during pyrolysis rather than originated from the sample since in SPME-GC-MS and wet-chemistry processes, we did not observe these numerous unsaturated products and few alkanes. These later few alkanes, however, observed with derivatization processes demonstrated their production by certain microbial populations in these extreme environments, see Tables 2 and 4.

On Mars with SAM experiments, we successfully detected alkanes up to C_{12} and carboxylic acid up to C_9 (and likely C_{12}), in addition to benzene and naphthalene (Eigenbrode et al., 2018; Szopa et al., 2020; Freissinet et al., 2015, 2019; Millan et al., 2016, 2022). In this analog study with hydrothermal vents that might mimic induced hydrothermal systems in the Gale crater investigated by MSL, we observed these low molecular weight organic compounds with, for most of them, a correlation with current life metabolisms. However, as a single molecule or without heavier organic compounds, we cannot extrapolate the detection of these gnostic biosignatures with potential past life on Mars since no strict biosignatures were noted in MSL analysis. First, because these compounds are produced abiotically as observed in meteoritic and returned asteroid samples (Cronin et al., 1993; Yuen and Kvenvolden, 1973; Becker et al., 1997; Schmitt-Kopplin et al., 2010). Second, on Mars, we did not detect heavy molecular weight compounds like peptidic or nucleic polymers or agnostic biosignatures (Eigenbrode et al., 2018; McAdam et al., 2014), such as a negative isotopic fractionation for carbon or nitrogen or co-localization of molecular biosignatures with nutrients or toxic elements trapped in a biofilm matrix

Table 4
Populations identified based on the lipidic and by-product metabolomic study performed in GC-MS (pyrolysis, TMAH and TMSH thermochemolysis).

Metabolites or biochemical families		Domain of life	Environmental adaptations
Lipids	FAMEs (>C23)	Few in all three	/
	FAMEs (<C23)	All three	/
	Unsaturated FAMEs	Eukaryote (and bacteria and archaea if monounsaturated)	Desaturases that elongate and desaturate saturated fatty acids: allow using free fatty acids by extracellular supply (1). The polyunsaturated fatty acids have important structural roles in cell membranes formation and integrity, but also physiology and signaling mechnaisms (3). They are also intermediates in biologically active molecules synthesis (*e.g.*, eicosanoids). Moreover, algae can produce the unsaturated acids by an aerobic and an anaerobic pathways, which is useful in extreme salty environments where water activity and oxygen content fluctuate according to the season. In our hot-springs, the anaerobic condition can be useful for algea being trapped in deep sinters (2). These are mostly useful for organelles in eukaryotes.
	(odd) Straight-chain FAMEs (fatty acids and fatty alcohols)	Eukaryote (and bacteria if < C23)	/
	Isoprenoid	Archaea	Extreme environments, especially halophiles for osmotic exchange and balance.
	Triglycerid	Eukaryotes	All for metabolic energy reserves.
	Fatty-acyl and diacylglycerol	Bacteria	/
	Diether phytanol-glycerol, archeol	Archaea primarily	Resistance to salty, highly thermal, and acidic biotopes, but do not synthesize fatty acids compared all other organisms to produce lipid membranes.
	Cyclopropane ring	Bacteria and few eukaryotes	/
Isoprenoid from pigments (chlorophyll, carotenoid)	Phytol hydrolysis	All three	Resistance to specific environments and use of light for energetic metabolism.
Sterols		Eukaryotes primarily and few bacteria	For membrane and eukaryotic organelles.
PAHs		Bacteria and eukaryotes primarily	By-products from lipid membrane, pigments.
Alkanes	Monomethyl	Bacteria	Cyanobacteria synthetize hydrocarbons through enzymatic modification of an elongated fatty acid (Coates et al., 2014). C17 n-alkane is specific to cyanobacteria branch.
Unsaturated compounds		Bacteria and eukaryotes	Thermophilic-metabolism.
S-compounds		All three	Sulfur-metabolism.
Phenol		Bacteria	Thermophilic-metabolism.
Polysaccharide		All three	Glyceraldehyde is reduced in glycerol that can be used for triglyceraldehyde stored in droplet form as metabolic energy reserves by bacteria and eukaryotes.
Hopanoid and steroid		Prokaryote and eukaryote, respectively	Rigidify the membrane for thermal resistance.

* few gram negative found in hot springs similar to Yellowstone Acidobacteriota, Aquificae, Bacteroidetes, Chloroflexia, Cyanobacteria, Pseudomonadota
** few gram positive have been found in similar Yellowstone samples to our hot springs: Actinomycetota
*** few thermoacidophiles have been found in similar Yellowstone samples to our hot springs.
(Thermoproteota and Thermoprotei orders) and Euryarchaeota archaeal branch, and Cyanidiales-Crenarchaeota archaeplastida eukaryote.

by organisms to feed or protect from their environment. The study of the first centimeters on Mars might be biased by the harsh oxidative and radiative environment that destroy evidence of potential past life traces (Hays et al., 2017; Pavlov et al., 2012, 2022).

Carboxylic acids of abiotic and fatty acids of biotic origin produce distinctly different profiles in GC-MS analyses, since, based on carboxylic acid abundance, the peak demonstrating the most abundant carbon-chain size in the Gaussian curve of acids distribution differ. The peak is around C_{16}-C_{18} for biotic origins (as noted in this study and previous works (Williams et al., 2021b; Blokker et al., 2002; Ishiwatari et al., 2006)) while the carbon ranges from C_1 – $C_{30\text{-}32}$ thanks to enzymatic elongations. On the opposite, abiotic processes do not reveal a carbon preference within the overall range from C_1 – $C_{8\text{-}12}$ (Cronin et al., 1993; Yuen and Kvenvolden, 1973). Moreover, we noticed a specific biosignature related to the shape of the main fatty acids detected, which were long straight chains of even carbon greater than the odd one due to enzymatically formed acetyl units (C_2) derived from glucose by the major species of Yellowstone hot-springs (Finkel et al., 2023; Loewen and Bindeman, 2016; Volkman and Volkman, 2006).

The lipidic analyses remain the most powerful tool in metabolomics studies to get a sense of the broad community diversity. Pyrolysis analyses helped first observe aromatics, alkanes, and alkenes that correlate with Raman observations. Indeed, the Raman bands were primarily due to lipids degradation. Second, TMAH and TMSH revealed the identification of 28 esters and three ethers present in GI Dig related to eukaryotic and bacterial populations. In contrast, the SG Dig exhibited a greater number of ethers and a distinct variety of esters, particularly those with heavy molecular weight fatty acids ranging from C_{16} to C_{30}. These compounds enable resistance to high temperatures, a characteristic typically associated with archaeal and hyperthermophilic bacteria classes (Table 2). On the opposite, in DI Active and Old, we noticed the light molecular weight straight chain fatty acids and two to three orders of magnitude higher in C_{16} and C_{18} (higher enrichment by 2–10 compared to the other samples) due to the phototrophic populations (Williams et al., 2021b) observed on the field and in SEM. In Dante's Inferno samples, C_{16} and C_{18} fatty acids (that are methylated by TMAH/TMSH to be detectable by GC-MS) were the most abundant in modern, compared to ancient precipitates. Indeed, a more diverse and abundant community was detected on the few samples analyzed in the modern towards the older samples demonstrating the quantity of C_{16} and C_{18} an order of magnitude higher in DI Active. Same conclusions for the increase in alkanes and PAHs in DI Old due to the degradation of microbial life and organic matter over hundreds to a thousand years by hydrothermal, erosion, temperature, and likely pH (according to SEM-EDX and Raman analysis coupled to GC-MS) parameters.

The untargeted environmental TMAH method allowed the detection and relative quantification of numerous sulfur-bearing compounds that are thio-metabolites – useful in the energetic and/or communication metabolisms of thermo/acidophilic extremophiles in SG Dig and GI Dig. The pyrite minerals are revealed by products formed in the pyrolyzer at 500 °C (*e.g.*, cyclic octaatomic sulfur). In addition, we detected few amines, alcohols, and aldehydes useful in the thermophilic-resistant

metabolism, such as phenols (*e.g.,* phenol, 3-methyl- or phenol, 2-methoxy-) that promotes electron transfer and are key to driving the humification of organic substances (Wen et al., 2022), 2,3,6-trio-O-methyl-galactopyranose involved in the energetic metabolism. We observed several primary metabolites produced by most of the organisms on Earth (*e.g.,* glyceraldehyde, 1H-indole-methyl, 1-methyl-5-oxo-proline), and few by-products of these microbial metabolites (*e.g.,* different alkanes (C_{16}-C_{44}), alkenes (C_2-C_6), aromatics and PAHs (C_6-C_{16})).

Therefore, the organic diversity revealed a part of the hot springs' community with about 50–150 compounds detected in each sample (Tables 2 and 4). 20–25% of these organic compounds are lipid-derivatives and 20–30% are by-products of lipids and other primary metabolites. Indeed, hydrothermal fluids alter, by oxidation and decarboxylation reactions the lipids, for instance, depicting a similar quantity of lipids and alkanes or aromatics. Some of these detected alkanes and aromatics are not only by-products of pyrolysis process or hydrothermal alterations, but also represent a secondary metabolites used to communicate between individuals, to feed or find nutrients, and/or to protect themselves like monomethyl alkanes in cyanobacteria. In addition, we noted the presence of several 1,2-di-O-alkylglycerols (diethers) and hopanoids characteristics of bacterial and archaeal metabolism and membranes (Kaur et al., 2008, 2011). As observed in previous studies, we also noticed that temperature (more than pH) tends to influence the length of hydrocarbon-chain for thermostability of the lipidic membrane above 40 °C, such as C_{16}-C_{20} to C_{20}-C_{30} straight fatty acids for hyperthermophiles or bacterial and archaeal diethers (Williams et al., 2021b; Kaur et al., 2015; Weerkamp and Heinen, 1972).

We detected the dominant archaeal lipids that include archaeol and glycerol dialkyl glycerol tetraethers (GDGTs) in high temperature hot springs towards thermophilic species (SG Dig, GI Dig, and in fewer quantity in DI Active to resist to acidic pH that might slightly vary seasonally even if the temperature does not vary) (Geilert et al., 2015a, 2015b; Holloway et al., 2011; Thomazo et al., 2009). In GI Dig, we discovered a lots of by-products coming from the mevalonate (MVA) pathway rather than the 2-C-methyl-D-erythritol 4-phosphate (MEB) pathway for the biosynthesis of isoprenoids. This observation leads to the hypothesis that the most acidic hot spring favors diversity in archaea and acidophilic bacteria lineage rather than in eukaryotic and gram-negative bacterial lineage (Chatzivasileiou et al., 2019; Koga and Morii, 2005; Robertson et al., 2005). The detection of some isoprenoids, mevalonate, and branched or multi-unsaturated alkenes (especially from three to five unsaturations are certain metabolites) due to decarboxylated fatty acids or terpenoids and isoprenoids degradation. These compounds could be a biosignature in Martian samples if they are detected along with their by-product derivatives. The strong degradation induced by volcanic/thermal and aqueous processes might explain why we did not observe phytol, or much archaeal membrane isoprenoids, steroids, hopanoids, and other terpenoids (Geilert et al., 2015a, 2015b; Holloway et al., 2011; Thomazo et al., 2009). The second reason for the absence of detection is the MS detection limits for these compounds and the low number of archaeal cells per mL (between 10^3 and 10^5 cells mL^{-1}). These isoprenoids similar to proteins are complex biosignatures that involve energetic and time-consuming production processes enhanced by catalytic metabolisms. Hence, they might not be detected abiotically, which is confirmed by the absence of detection in meteorites and returned samples. To detect these biotic-driven molecules, the quantity of cells in collected extraterrestrial samples should be higher than 10^5 cells mL^{-1} for MS detection by pyrolysis or thermochemolysis (Boulesteix et al., 2022).

Biomolecules/by-products as a whole (that are not produced abiotically) might represent a "biosignature", which could reveal the presence of primitive archaea and/or gram-positive bacteria in extraterrestrial samples, since they are both the main populations in hydrothermal systems and what we think as being the first populations on the Early-Earth (Euryarchaeota, DPANN, and likely Asgard and TACK superphyla) (Giulio, 2003; Cantine and Fournier, 2018). The lipid content was similar in all samples except for diethers, sterols, GDGTs, glycolipids, and sugars. We also found biomolecules that have different metabolic roles, such as N-(-2-acetamido)iminodiacetic acid (cellular buffer), amino acids (protein bases and secondary metabolites), nucleobases (DNA and RNA bases), and S-bearing compounds like carbonimidodithioic acid, methyl- (that might be secondary metabolite products). In pyrolysis at 600 °C, we also observed the degradation of all microbial metabolites with alkanes and alkenes ranging from C_{10} to $C_{20\text{-}22}$ (with a greater abundance from C_{16} to C_{20} from bacterial populations) with an even-over-odd predominance. Indeed, odd organic compounds ranged only between C_{15} and C_{23} two to ten times lower in abundance compared to the even compounds. This even-over-odd predominance has been observed for alkanes, alkenes, and methylated fatty acids in TMAH and TMSH experiments. This disruptive length of skeleton carbons is related to Earth life microbes that favored mid-chain lipids for robustness and adaptive selection to achieve osmotic balance, inter and intra-population communication or quorum sensing, and nutrients absorption. We identified monomethyl alkanes (*e.g.,* n-nonomethylhexadecane and n-monomethylheptadecane) like in previous Yellowstone hot springs that recorded the presence of cyanobacteria (Shiea et al., 1991), and longer-chain fatty acids and saturated components are more abundant at higher temperatures consistent with literature for thermostability and/or acidophilic metabolisms for osmotic equilibrium and preserve a neutral-alkaline state in cells to have phosphate and other nutrients at the base state (Harwood, 2012; Weerkamp and Heinen, 1972; Harwood et al., 1984).

Hence, the metabolites segregated three different communities for the three different hot springs due primarily to temperature and pH of the distal apron sinters collected: i) (hyper-)thermophiles' community in the 'Similar geyser' (SG Dig) hot-spring with numerous ether bonds (*e.g.,* octanoic acid, methoxy-, 8-dodecenoic acid, methoxy-, and hexadecanoic acid, methoxy-) belonging to archaeal membranes and few bacterial domains of life (such as *Aquificales* (Pancost et al., 2005; Jain et al., 2014)) including dialkyl glycerol diethers (DGDs) and dialkyl glycerol tetraethers (GDGTs) for membrane stabilization in hot waters (Koga, 2012; Albers et al., 2000; van der Meer et al., 2010), ii) mesophiles, thermotolerants, and acidophiles form a community in the 'Goldilocks' (GI Dig), and iii) neutrophile to alkalinophile thermophilic populations at Dante's Inferno (DI Active and DI Old) hot springs, presenting specific features, such as monomethyl and long-chain unsaturated alkanes and alkenes (from *Chloroflexi* (van der Meer et al., 2000; Frese et al., 1997; Goossens et al., 1984)), linear isoprenoids (from *Cyanobacteria* (Didyk et al., 1978; Parenteau et al., 2014; Geilert et al., 2015a)), and by-products of pigments for bacterial and oxygenic phototrophs (where symbiotic association between *Cyanobacteria* and *Chloroflexi* within collected microbial mats).

5. Conclusions

Mars has been visited multiple times at multiple locations representing different types of environments. The future explorations by the Mars rovers of ancient volcanic systems may give clues to detect complex and heavy organic compounds on Mars. Silica sinters preserve organic matter and fossils from UV radiation over a long period of time (millions to billions of years). In addition, volcanic systems are full of features and specific signatures that are preserved over billions of years after the inactivity of the system. Therefore, to predict the type of bioindicators, biosignatures, or geophysical features we are looking for on Mars, we visited Mars analog volcanic-hydrothermal systems. Three sites across Yellowstone National Park (WY, USA) were selected for sampling based on criteria of temperature (above and below the upper limit for photosynthesis and microalgae survival, *i.e.,* 72 °C), pH (acidic to alkaline), and low to very low biomass (from 0.1 to 1 % in TOC by dry weight) for Mars relevance according to the different past very active volcanic areas observed and/or explored by rovers/landers (Viking,

Spirit, Phoenix, Curiosity, Perseverance, and in the future Rosalind Franklin). We confirmed previous results observed in other studies that primarily lipid biomarkers are well preserved in geothermal sinters due to a rapid silicification (Pancost et al., 2005; Kaur et al., 2008, 2011; Gibson et al., 2014).

The different signatures detected across the study can be gathered into three groups: i) the geophysical linked to geobiological features (*i.e.,* pyrite associated to biofilm or degraded EPS molecules; ii) the geochemical signatures (*i.e.,* correlation of uncommon isotopy for carbon, nitrogen, and sulfur compared to the average isotopic ratio on Mars); correlation between the concentration in organic matter and specific elements such as sulfates, carbonates, arsenic, cesium; and iii) degraded or intact heavy molecular organic compounds such as PAHs, alkanes, and lipids, sugars and alcohols, amino acids and amines; a ratio C_{24}-C_{30}/C_1-C_{20} equivalent to Mars analog found in Yellowstone and on Earth volcanic systems; the degraded pattern and compounds of lipids relative to the one known on Earth after few million to billions of years. We can extrapolate to all hot spring systems on Earth and potentially to Mars that we have three types of communities according to the range of temperature and pH: i) acidophilic and (hyper)thermophilic communities constituted mostly by *Chloroflexi*, *Actinobacteria*, *Sulfolobales*, *Geoarchaeales*, and few populations of sulfo-oxidizers (and in the distal-apron sinters oxygenic photosynthetizers like green algae); ii) neutral and ambient temperature with *Proteobacteria*, *Aquificae*, few *Thermoproteales*, and *Desulfurococcales*; and iii) alkaline and (hyper)thermophilic hot springs where chemotrophic and thermophilic populations thrive, notably *Chloroflexi*, *Aquificae*, hyperthermophilic archaea, and in the distal-apron area *Cyanobacteria*, and few fungi, diatoms, oxygenic and anoxic photosynthetizers. Therefore, for future Mars explorations and return sample analysis we should investigate the molecular and potentially microbial signatures connected to these populations.

There were robust microbial communities living in and on the siliceous deposits/in the hot springs for each of these environments. Indeed, by comparing siliceous sinters from these different geochemical environments provides evidence for how the extant microbial communities (and/or signals generated by them) are preserved within the silica precipitated at the different sites - which is critical to communicate to the planetary community, since all of the siliceous sinters have physical evidence of life (as well as geochemical). This helps to show that any hot spring siliceous sinter deposit that is found on Mars should absolutely be studied in depth. Therefore, in our Early diagenesis processing samples, we proved the higher preservation rate of microbial communities in acidic environment on the opposite of alkaline hot springs (on the opposite of the first insight and hypothesis we may have where alkaline springs support the production of different minerals that might help the fossilization or preservation of cells like sulfates). The results lead to a second new conclusion that must be verified on further hot springs in Mars analog environments regarding the degradation of past or current life traces in neutral to alkaline silica sinters before diagenesis process meaning the implication of most probably chemical interactions with the organic compounds that degrades faster or as fast as the diagenesis process. Therefore, on Mars, we should study past and/or present acidic silica sinters and volcanic sites to detect organic compounds from samples dating back billions of years.

CRediT authorship contribution statement

D. Boulesteix: Writing – original draft, Visualization, Validation, Methodology, Investigation, Funding acquisition, Formal analysis, Conceptualization. **A. Buch:** Writing – review & editing, Validation, Supervision, Software, Resources, Project administration, Methodology, Funding acquisition. **G. Masson:** Formal analysis. **L.L. Kivrak:** Data curation. **J.R. Havig:** Writing – review & editing. **T.L. Hamilton:** Writing – review & editing. **B.L. Teece:** Writing – review & editing, Resources. **Y. He:** Writing – review & editing, Validation. **C. Freissinet:** Writing – review & editing. **Y. Huang:** Writing – review & editing, Supervision, Methodology. **E. Santos:** Writing – review & editing, Methodology, Formal analysis. **C. Szopa:** Writing – review & editing. **A. J. Williams:** Writing – review & editing, Validation, Supervision, Software, Resources, Project administration, Methodology, Conceptualization.

Declaration of competing interest

The authors declare the following financial interests/personal relationships which may be considered as potential competing interests: Boulesteix David reports travel was provided by Fulbright. Boulesteix David reports a relationship with CentraleSupélec that includes: funding grants. If there are other authors, they declare that they have no known competing financial interests or personal relationships that could have appeared to influence the work reported in this paper.

Data availability

Data will be made available on request.

Acknowledgment

Accreditation from Yellowstone National park, and the collaborators that help collect samples and analyze data. A portion of this work was conducted at the Jet Propulsion Laboratory, California Institute of Technology under a contract with the National Aeronautics and Space Administration (80NM0018D0004). We also would like to thanks Fulbright for the Student-Research grant. And we thank the scientists in UF (Jason Curtis, John M. Jaeger, Alison A. Trachet, George Kamenov, Jay Dynes, Kristy Schepker, and Stephen M. Elardo) and CentraleSupélec-UPS (Pascale Gemeiner). The decision to implement Mars Sample Return and the Rosalind Franklin rover mission will not be finalized until NASA's completion of the National Environmental Policy Act (NEPA) process. This document is being made available for information purposes only.

Appendix A. Supplementary data

Supplementary data to this article can be found online at https://doi.org/10.1016/j.pss.2024.105953.

References

Abramov, O., Kring, D.A., 2005. Impact-induced hydrothermal activity on early Mars. J. Geophys. Res.: Planets 110. https://doi.org/10.1029/2005JE002453.

Albers, S.-V., van de Vossenberg, J.L.C.M., Driessen, A.J.M., Konings, W.N., 2000. Adaptations of the archaeal cell membrane to heat stress. FBL 5, 813–820. https://doi.org/10.2741/albers.

Alwmark, S., et al., 2023. Diverse lava flow morphologies in the stratigraphy of the Jezero Crater Floor. Journal of Geophysical Research. Planets, e2022JE007446.

Archer, P.D., et al., 2014. Abundances and implications of volatile-bearing species from evolved gas analysis of the Rocknest aeolian deposit, Gale Crater, Mars. J. Geophys. Res. Planets 119, 237–254. https://doi.org/10.1002/2013JE004493.

Aubrey, A., et al., 2006. Sulfate minerals and organic compounds on Mars. Geol. 34, 357. https://doi.org/10.1130/G22316.1.

Becker, L., Glavin, D.P., Bada, J.L., 1997. Polycyclic aromatic hydrocarbons (PAHs) in Antarctic Martian meteorites, carbonaceous chondrites, and polar ice. Geochem. Cosmochim. Acta 61, 475–481. https://doi.org/10.1016/S0016-7037(96)00400-0.

Bibring, J.-P., Hamm, V., Pilorget, C., Vago, J.L., 2017. The MicrOmega investigation onboard ExoMars. Astrobiology 17, 621–626. https://doi.org/10.1089/ast.2016.1642.

Biemann, K., 2007. On the ability of the Viking gas chromatograph–mass spectrometer to detect organic matter. Proc. Natl. Acad. Sci. USA 104, 10310–10313. https://doi.org/10.1073/pnas.0703732104.

Biemann, K., et al., 1977. The search for organic substances and inorganic volatile compounds in the surface of Mars. J. Geophys. Res. 82, 4641–4658. https://doi.org/10.1029/JS082i028p04641.

Bindeman, I.N., Valley, J.W., 2000. Formation of low-δ18O rhyolites after caldera collapse at Yellowstone, Wyoming, USA. Geology 28, 719–722. https://doi.org/10.1130/0091-7613(2000)28<719:FOLRAC>2.0.CO;2.

Blokker, P., Pel, R., Akoto, L., Brinkman, U.A.Th, Vreuls, R.J.J., 2002. At-line gas chromatographic–mass spectrometric analysis of fatty acid profiles of green

microalgae using a direct thermal desorption interface. J. Chromatogr. A 959, 191–201. https://doi.org/10.1016/S0021-9673(02)00463-6.
Boulesteix, D., Buch, A., Szopa, C., He, Y., Freissinet, C., Coscia, D., 2022. Extremophile Metabolite Study to Detect Potential Biosignatures and Interpret Future Gas Chromatography-Mass spectrometry Ocean Worlds in situ analysis (e.g. Dragonfly mission with its DraMS instrument and EuropaLander with its EMILI instrument). In: AGU Fall Meeting Abstracts, pp. P55G–P1650.
Boynton, W.V., et al., 2001. Thermal and evolved gas analyzer: Part of the mars volatile and climate surveyor integrated payload. J. Geophys. Res. 106, 17683–17698. https://doi.org/10.1029/1999JE001153.
Brabandere, L.D., Frazer, T.K., Montoya, J.P., 2007. Stable nitrogen isotope ratios of macrophytes and associated periphyton along a nitrate gradient in two subtropical, spring-fed streams. Freshw. Biol. 52, 1564–1575. https://doi.org/10.1111/j.1365-2427.2007.01788.x.
Brown, A.J., Viviano, C.E., Goudge, T.A., 2020. Olivine-carbonate mineralogy of the Jezero crater region. J. Geophys. Res.: Planets 125, e2019JE006011.
Buch, A., et al., 2022. Influence of the secondary X-Rays on the organic matter at Mars' near-surface. AGU Fall Meeting Abstracts 2022. P12A-08.
Bundschuh, J., Maity, J.P., 2015. Geothermal arsenic: occurrence, mobility and environmental implications. Renew. Sustain. Energy Rev. 42, 1214–1222. https://doi.org/10.1016/j.rser.2014.10.092.
S.L. Cady, J.D. Farmer, Fossilization Processes in Siliceous Thermal Springs: Trends in Preservation Along Thermal Gradients, in: Ciba Foundation Symposium 202 - Evolution of Hydrothermal Ecosystems on Earth (And Mars?), John Wiley & Sons, Ltd, n.d.: pp. 150–173. https://doi.org/10.1002/9780470514986.ch9.
Campbell, K.A., Guido, D.M., Gautret, P., Foucher, F., Ramboz, C., Westall, F., 2015. Geyserite in hot-spring siliceous sinter: window on Earth's hottest terrestrial (paleo) environment and its extreme life. Earth Sci. Rev. 148, 44–64. https://doi.org/10.1016/j.earscirev.2015.05.009.
Cantine, M.D., Fournier, G.P., 2018. Environmental adaptation from the origin of life to the last universal common ancestor. Orig. Life Evol. Biosph. 48, 35–54. https://doi.org/10.1007/s11084-017-9542-5.
Carr, M.H., 1996. Water on Mars. Oxford University Press. https://doi.org/10.1093/oso/9780195099386.001.0001.
Carrier, B.L., Kounaves, S.P., 2015. The origins of perchlorate in the Martian soil. Geophys. Res. Lett. 42, 3739–3745. https://doi.org/10.1002/2015GL064290.
Carruthers, D.N., Lee, T.S., 2021. Diversifying isoprenoid platforms via atypical carbon substrates and non-model microorganisms. Front. Microbiol. 12.
Carter, J., Quantin, C., Thollot, P., Loizeau, D., Ody, A., Lozach, L., 2016. Oxia Planum: A Clay-Laden Landing Site Proposed for the ExoMars Rover Mission: Aqueous Mineralogy and Alteration Scenarios, p. 2064.
Carter, J., Riu, L., Poulet, F., Bibring, J.-P., Langevin, Y., Gondet, B., 2023. A Mars orbital catalog of aqueous alteration signatures (MOCAAS). Icarus 389, 115164.
Casero, M.C., Ascaso, C., Quesada, A., Mazur-Marzec, H., Wierzchos, J., 2021. Response of endolithic chroococcidiopsis strains from the polyextreme Atacama desert to light radiation. Front. Microbiol. 11. https://www.frontiersin.org/articles/10.3389/fmicb.2020.614875.
Chatzivasileiou, A.O., Ward, V., Edgar, S.M., Stephanopoulos, G., 2019. Two-step pathway for isoprenoid synthesis. Proc. Natl. Acad. Sci. U. S. A. 116, 506–511. https://doi.org/10.1073/pnas.1812935116.
Clark, B.C., Kounaves, S.P., 2016. Evidence for the distribution of perchlorates on Mars. Int. J. Astrobiol. 15, 311–318. https://doi.org/10.1017/S1473550415000385.
Clark, J., et al., 2021. A review of sample analysis at mars-evolved gas analysis laboratory analog work supporting the presence of perchlorates and chlorates in Gale Crater, mars. Minerals 11, 475. https://doi.org/10.3390/min11050475.
Corpolongo, A., et al., 2023. SHERLOC Raman mineral class detections of the mars 2020 crater floor campaign. J. Geophys. Res.: Planets 128, e2022JE007455. https://doi.org/10.1029/2022JE007455.
Crits-Christoph, A., et al., 2013. Colonization patterns of soil microbial communities in the Atacama Desert. Microbiome 1, 28. https://doi.org/10.1186/2049-2618-1-28.
Cronin, J.R., Pizzarello, S., Epstein, S., Krishnamurthy, R.V., 1993. Molecular and isotopic analyses of the hydroxy acids, dicarboxylic acids, and hydroxydicarboxylic acids of the Murchison meteorite. Geochem. Cosmochim. Acta 57, 4745–4752. https://doi.org/10.1016/0016-7037(93)90197-5.
Darma, A., Yang, J., Bloem, E., Możdżen, K., Zandi, P., 2022. Arsenic biotransformation and mobilization: the role of bacterial strains and other environmental variables. Environ. Sci. Pollut. Res. 29, 1763–1787. https://doi.org/10.1007/s11356-021-17117-x.
Didyk, B.M., Simoneit, B.R.T., Brassell, S.C., Eglinton, G., 1978. Organic geochemical indicators of palaeoenvironmental conditions of sedimentation. Nature 272, 216–222. https://doi.org/10.1038/272216a0.
Djokic, T., Van Kranendonk, M.J., Campbell, K.A., Walter, M.R., Ward, C.R., 2017. Earliest signs of life on land preserved in ca. 3.5 Ga hot spring deposits. Nat. Commun. 8, 15263 https://doi.org/10.1038/ncomms15263.
dos Santos, R., Patel, M., Cuadros, J., Martins, Z., 2016. Influence of mineralogy on the preservation of amino acids under simulated Mars conditions. Icarus 277, 342–353. https://doi.org/10.1016/j.icarus.2016.05.029.
Eigenbrode, J.L., et al., 2018. Organic matter preserved in 3-billion-year-old mudstones at Gale crater, Mars. Science 360, 1096–1101. https://doi.org/10.1126/science.aas9185.
Fawdon, P., et al., 2024. The high-resolution map of Oxia Planum, Mars; the landing site of the ExoMars Rosalind Franklin rover mission. J. Maps 20 (1). https://doi.org/10.1080/17445647.2024.2302361.
Ferrari, M., De Angelis, S., De Sanctis, M.C., Frigeri, A., Altieri, F., Ammannito, E., Formisano, M., Vinogradoff, V., 2023. Constraining the Rosalind Franklin rover/ma_MISS instrument capability in the detection of organics. Astrobiology 23, 691–704.
Finkel, P.L., Carrizo, D., Parro, V., Sánchez-García, L., 2023. An overview of lipid biomarkers in terrestrial extreme environments with relevance for mars exploration. Astrobiology 23, 563–604. https://doi.org/10.1089/ast.2022.0083.
François, P., et al., 2016. Magnesium sulfate as a key mineral for the detection of organic molecules on Mars using pyrolysis: mg sulfate effect on organic pyrolysis. J. Geophys. Res. Planets 121, 61–74. https://doi.org/10.1002/2015JE004884.
Franz, H.B., et al., 2017. Large sulfur isotope fractionations in Martian sediments at Gale crater. Nat. Geosci. 10, 658–662. https://doi.org/10.1038/ngeo3002.
Freissinet, C., et al., 2015. Organic molecules in the sheepbed mudstone, Gale Crater, mars: detection of organics in martian sample. J. Geophys. Res. Planets 120, 495–514. https://doi.org/10.1002/2014JE004737.
Freissinet, C., et al., 2019. Detection of Long-Chain Hydrocarbons on Mars with the Sample Analysis at Mars (SAM) Instrument, vol. 2089, p. 6123.
Frese, R., Oberheide, U., van Stokkum, I., van Grondelle, R., Foidl, M., Oelze, J., van Amerongen, H., 1997. The organization of bacteriochlorophyll c in chlorosomes from Chloroflexus aurantiacus and the structural role of carotenoids and protein. Photosynth. Res. 54, 115–126. https://doi.org/10.1023/A:1005903613179.
Frydenvang, J., et al., 2017. Diagenetic silica enrichment and late-stage groundwater activity in Gale crater, Mars. Geophys. Res. Lett. 44, 4716–4724. https://doi.org/10.1002/2017GL073323.
Gago, G., Diacovich, L., Arabolaza, A., Tsai, S.-C., Gramajo, H., 2011. Fatty acid biosynthesis in actinomycetes. FEMS Microbiol. Rev. 35, 475–497. https://doi.org/10.1111/j.1574-6976.2010.00259.x.
Gainey, S.R., Elwood Madden, M.E., 2012. Kinetics of methane clathrate formation and dissociation under Mars relevant conditions. Icarus 218, 513–524. https://doi.org/10.1016/j.icarus.2011.12.019.
Gainey, S.R., et al., 2017. Clay mineral formation under oxidized conditions and implications for paleoenvironments and organic preservation on Mars. Nat. Commun. 8, 1230. https://doi.org/10.1038/s41467-017-01235-7.
Gangidine, A., Havig, J.R., Fike, D.A., Jones, C., Hamilton, T.L., Czaja, A.D., 2020. Trace element concentrations in hydrothermal silica deposits as a potential biosignature. Astrobiology 20, 525–536. https://doi.org/10.1089/ast.2018.1994.
Geilert, S., Vroon, P.Z., Keller, N.S., Gudbrandsson, S., Stefánsson, A., van Bergen, M.J., 2015a. Silicon isotope fractionation during silica precipitation from hot-spring waters: evidence from the Geysir geothermal field, Iceland. Geochem. Cosmochim. Acta 164, 403–427. https://doi.org/10.1016/j.gca.2015.05.043.
Geilert, S., Vroon, P.Z., Keller, N.S., Gudbrandsson, S., Stefánsson, A., van Bergen, M.J., 2015b. Silicon isotope fractionation during silica precipitation from hot-spring waters: evidence from the Geysir geothermal field, Iceland. Geochem. Cosmochim. Acta 164, 403–427. https://doi.org/10.1016/j.gca.2015.05.043.
Gibson, R.A., Sherry, A., Kaur, G., Pancost, R.D., Talbot, H.M., 2014. Bacteriohopanepolyols preserved in silica sinters from Champagne Pool (New Zealand) indicate a declining temperature gradient over the lifetime of the vent. Org. Geochem. 69, 61–69. https://doi.org/10.1016/j.orggeochem.2014.02.004.
Gihring, T.M., Banfield, J.F., 2001. Arsenite oxidation and arsenate respiration by a new Thermus isolate. FEMS (Fed. Eur. Microbiol. Soc.) Microbiol. Lett. 204, 335–340. https://doi.org/10.1111/j.1574-6968.2001.tb10907.x.
Gillen, C., Jeancolas, C., McMahon, S., Vickers, P., 2023. The call for a new definition of biosignature. Astrobiology 23, 1228–1237. https://doi.org/10.1089/ast.2023.0010.
Giulio, M.D., 2003. The universal ancestor was a thermophile or a hyperthermophile: tests and further evidence. J. Theor. Biol. 221, 425–436. https://doi.org/10.1006/jtbi.2003.3197.
Glavin, D.P., et al., 2013. Evidence for perchlorates and the origin of chlorinated hydrocarbons detected by SAM at the Rocknest aeolian deposit in Gale Crater: evidence for Perchlorates at Rocknest. J. Geophys. Res. Planets 118, 1955–1973. https://doi.org/10.1002/jgre.20144.
Goesmann, F., et al., 2017. The mars organic molecule analyzer (MOMA) instrument: characterization of organic material in martian sediments. Astrobiology 17, 655–685. https://doi.org/10.1089/ast.2016.1551.
Goetz, W., et al., 2016. MOMA: the challenge to search for organics and biosignatures on Mars. Int. J. Astrobiol. 15, 239–250. https://doi.org/10.1017/S1473550416000227.
Golombek, M., et al., 2012. Selection of the mars science laboratory landing site. Space Sci. Rev. 170, 641–737. https://doi.org/10.1007/s11214-012-9916-y.
Gonsior, M., Hertkorn, N., Hinman, N., Dvorski, S.E.-M., Harir, M., Cooper, W.J., Schmitt-Kopplin, P., 2018. Yellowstone hot springs are organic chemodiversity hot spots. Sci. Rep. 8, 14155 https://doi.org/10.1038/s41598-018-32593-x.
Goossens, H., de Leeuw, J.W., Schenck, P.A., Brassell, S.C., 1984. Tocopherols as likely precursors of pristane in ancient sediments and crude oils. Nature 312, 440–442. https://doi.org/10.1038/312440a0.
Goudge, T.A., Milliken, R.E., Head, J.W., Mustard, J.F., Fassett, C.I., 2017. Sedimentological evidence for a deltaic origin of the western fan deposit in Jezero crater, Mars and implications for future exploration. Earth Planet Sci. Lett. 458, 357–365. https://doi.org/10.1016/j.epsl.2016.10.056.
Grotzinger, J., Al-Rawahi, Z., 2014. Depositional facies and platform architecture of microbialite-dominated carbonate reservoirs, Ediacaran–Cambrian Ara Group, Sultanate of Oman. AAPG (Am. Assoc. Pet. Geol.) Bull. 98, 1453–1494. https://doi.org/10.1306/02271412063.
Grotzinger, J.P., et al., 2012. Mars science laboratory mission and science investigation. Space Sci. Rev. 170, 5–56. https://doi.org/10.1007/s11214-012-9892-2.
Hamilton, T.L., Bennett, A.C., Murugapiran, S.K., Havig, J.R., 2019. Anoxygenic phototrophs span geochemical gradients and diverse morphologies in terrestrial geothermal springs. mSystems 4. https://doi.org/10.1128/msystems.00498-19, 10.1128/msystems.00498-19.
Hanson, M.C., Oze, C., Werner, C., Horton, T.W., 2018. Soil δ13C-CO2 and CO2 flux in the H2S-rich rotorua hydrothermal system utilizing cavity ring down spectroscopy.

J. Volcanol. Geoth. Res. 358, 252–260. https://doi.org/10.1016/j.jvolgeores.2018.05.018.
Harwood, J., 2012. Lipids in Plants and Microbes. Springer Science & Business Media.
Harwood, J.L., Russell, N.J., 1984. Introduction. In: Harwood, J.L., Russell, N.J. (Eds.), Lipids in Plants and Microbes. Springer Netherlands, Dordrecht, pp. 1–6. https://doi.org/10.1007/978-94-011-5989-0_1.
Hassler, D.M., et al., 2014a. Mars' surface radiation environment measured with the Mars Science Laboratory's Curiosity rover. Science 343, 1244797.
Hassler, D.M., et al., 2014b. Mars' surface radiation environment measured with the mars science laboratory's curiosity rover. Science 343, 1244797. https://doi.org/10.1126/science.1244797.
Havig, J.R., Hamilton, T.L., 2019a. Hypolithic photosynthesis in hydrothermal areas and implications for cryptic oxygen oases on archean continental surfaces. Front. Earth Sci. 7. https://www.frontiersin.org/articles/10.3389/feart.2019.00015.
Havig, J.R., Hamilton, T.L., 2019b. Productivity and community composition of low biomass/high silica precipitation hot springs: a possible window to earth's early biosphere? Life 9, 64. https://doi.org/10.3390/life9030064.
Havig, J.R., Raymond, J., Meyer-Dombard, D.R., Zolotova, N., Shock, E.L., 2011. Merging isotopes and community genomics in a siliceous sinter-depositing hot spring. J. Geophys. Res.: Biogeosciences 116. https://doi.org/10.1029/2010JG001415.
Havig, J.R., Kuether, J.E., Gangidine, A.J., Schroeder, S., Hamilton, T.L., 2021. Hot spring microbial community elemental composition: hot spring and soil inputs, and the transition from biocumulus to siliceous sinter. Astrobiology 21, 1526–1546. https://doi.org/10.1089/ast.2019.2086.
Hays, L.E., 2015. NASA Astrobiology Strategy 2015.
Hays, L.E., et al., 2017. Biosignature preservation and detection in mars analog environments. Astrobiology 17, 363–400. https://doi.org/10.1089/ast.2016.1627.
Hewelt-Belka, W., Kot-Wasik, A., Tamagnini, P., Oliveira, P., 2020. Untargeted lipidomics analysis of the cyanobacterium synechocystis sp. PCC 6803: lipid composition variation in response to alternative cultivation setups and to gene deletion. Int. J. Mol. Sci. 21, 8883. https://doi.org/10.3390/ijms21238883.
Holloway, J.M., Nordstrom, D.K., Böhlke, J.K., McCleskey, R.B., Ball, J.W., 2011. Ammonium in thermal waters of Yellowstone National Park: processes affecting speciation and isotope fractionation. Geochem. Cosmochim. Acta 75, 46114636. https://doi.org/10.1016/j.gca.2011.05.036.
Hurwitz, S., Lowenstern, J.B., 2014. Dynamics of the Yellowstone hydrothermal system. Rev. Geophys. 52, 375–411. https://doi.org/10.1002/2014RG000452.
Ishiwatari, R., Yamamoto, S., Shinoyama, S., 2006. Lignin and fatty acid records in Lake Baikal sediments over the last 130kyr: a comparison with pollen records. Org. Geochem. 37, 1787–1802. https://doi.org/10.1016/j.orggeochem.2006.10.005.
Jahnke, L.L., Eder, W., Huber, R., Hope, J.M., Hinrichs, K.U., Hayes, J.M., Des Marais, D. J., Cady, S.L., Summons, R.E., 2001. Signature lipids and stable carbon isotope analyses of Octopus Spring hyperthermophilic communities compared with those of Aquificales representatives. Appl. Environ. Microbiol. 67, 5179–5189. https://doi.org/10.1128/AEM.67.11.5179-5189.2001.
Jain, S., Caforio, A., Driessen, A.J.M., 2014. Biosynthesis of archaeal membrane ether lipids. Front. Microbiol. 5. https://www.frontiersin.org/articles/10.3389/fmicb.2014.00641.
Jones, B., 2021. Siliceous sinters in thermal spring systems: review of their mineralogy, diagenesis, and fabrics. Sediment. Geol. 413, 105820 https://doi.org/10.1016/j.sedgeo.2020.105820.
Kaur, G., Mountain, B.W., Pancost, R.D., 2008. Microbial membrane lipids in active and inactive sinters from Champagne Pool, New Zealand: elucidating past geothermal chemistry and microbiology. Org. Geochem. 39, 1024–1028. https://doi.org/10.1016/j.orggeochem.2008.04.016.
Kaur, G., Mountain, B.W., Hopmans, E.C., Pancost, R.D., 2011. Preservation of microbial lipids in geothermal sinters. Astrobiology 11, 259–274. https://doi.org/10.1089/ast.2010.0540.
Kaur, G., Mountain, B.W., Stott, M.B., Hopmans, E.C., Pancost, R.D., 2015. Temperature and pH control on lipid composition of silica sinters from diverse hot springs in the Taupo Volcanic Zone, New Zealand. Extremophiles 19, 327–344. https://doi.org/10.1007/s00792-014-0719-9.
Klein, H.P., Lederberg, J., Rich, A., Horowitz, N.H., Oyama, V.I., Levin, G.V., 1976. The viking mission search for life on mars. Nature 262, 24–27. https://doi.org/10.1038/262024a0.
Kminek, G., Bada, J., 2006. The effect of ionizing radiation on the preservation of amino acids on Mars. Earth Planet Sci. Lett. 245, 1–5. https://doi.org/10.1016/j.epsl.2006.03.008.
Knak Jensen, S.J., et al., 2014. A sink for methane on Mars? The answer is blowing in the wind. Icarus 236, 24–27. https://doi.org/10.1016/j.icarus.2014.03.036.
Koga, Y., 2012. Thermal adaptation of the archaeal and bacterial lipid membranes. Archaea 2012, 789652. https://doi.org/10.1155/2012/789652.
Koga, Y., Morii, H., 2005. Recent advances in structural research on ether lipids from archaea including comparative and physiological aspects. Biosci., Biotechnol., Biochem. 69, 2019–2034. https://doi.org/10.1271/bbb.69.2019.
Kumari, P., Kumar, M., Reddy, C.R.K., Jha, B., 2013. 3 - algal lipids, fatty acids and sterols. In: Domínguez, H. (Ed.), Functional Ingredients from Algae for Foods and Nutraceuticals. Woodhead Publishing, pp. 87–134. https://doi.org/10.1533/9780857098689.1.87.
Lamed, R.J., Zeikus, J.G., 1981. Novel NADP-linked alcohol–aldehyde/ketone oxidoreductase in thermophilic ethanologenic bacteria. Biochem. J. 195, 183–190. https://doi.org/10.1042/bj1950183.
Lewis, J.M.T., Watson, J.S., Najorka, J., Luong, D., Sephton, M.A., 2015. Sulfate minerals: a problem for the detection of organic compounds on mars? Astrobiology 15, 247–258. https://doi.org/10.1089/ast.2014.1160.
Loewen, M.W., Bindeman, I.N., 2016. Oxygen isotope thermometry reveals high magmatic temperatures and short residence times in Yellowstone and other hot-dry rhyolites compared to cold-wet systems. Am. Mineral. 101, 1222–1227. https://doi.org/10.2138/am-2016-5591.
Haridon, J.L., et al., 2020. Iron mobility during diagenesis at vera rubin ridge, Gale Crater, mars. J. Geophys. Res.: Planets 125, e2019JE006299. https://doi.org/10.1029/2019JE006299.
Mahaffy, P.R., et al., 2012. The sample analysis at mars investigation and instrument suite. Space Sci. Rev. 170, 401–478. https://doi.org/10.1007/s11214-012-9879-z.
Mangold, N., et al., 2020. Fluvial regimes, morphometry, and age of Jezero Crater paleolake inlet valleys and their exobiological significance for the 2020 rover mission landing site. Astrobiology 20, 994–1013. https://doi.org/10.1089/ast.2019.2132.
McAdam, A.C., et al., 2014. Sulfur-bearing phases detected by evolved gas analysis of the Rocknest aeolian deposit, Gale Crater, Mars: rocknest sulfur phases detected by SAM. J. Geophys. Res. Planets 119, 373–393. https://doi.org/10.1002/2013JE004518.
Millan, M., et al., 2016. In situ analysis of martian regolith with the SAM experiment during the first mars year of the MSL mission: identification of organic molecules by gas chromatography from laboratory measurements. Planet. Space Sci. 129, 88–102. https://doi.org/10.1016/j.pss.2016.06.007.
Millan, M., et al., 2022. Organic molecules revealed in Mars's Bagnold Dunes by Curiosity's derivatization experiment. Nat. Astron. 6, 129–140. https://doi.org/10.1038/s41550-021-01507-9.
Miller, K.E., Eigenbrode, J.L., Freissinet, C., Glavin, D.P., Kotrc, B., Francois, P., Summons, R.E., 2016. Potential precursor compounds for chlorohydrocarbons detected in Gale Crater, mars, by the SAM instrument suite on the curiosity rover: precursors of martian chlorohydrocarbons. J. Geophys. Res. Planets 121, 296–308. https://doi.org/10.1002/2015JE004939.
Mumma, M.J., et al., 2009. Strong release of methane on mars in northern summer 2003. Science 323, 1041–1045. https://doi.org/10.1126/science.1165243.
Navarro-Gonzalez, R., 2003. Mars-like soils in the Atacama desert, Chile, and the dry limit of microbial life. Science 302, 1018–1021. https://doi.org/10.1126/science.1089143.
Navarro-Gonzalez, R., et al., 2006. The limitations on organic detection in Mars-like soils by thermal volatilization-gas chromatography-MS and their implications for the Viking results. Proc. Natl. Acad. Sci. USA 103, 16089–16094. https://doi.org/10.1073/pnas.0604210103.
Neveu, M., Hays, L.E., Voytek, M.A., New, M.H., Schulte, M.D., 2018. The ladder of life detection. Astrobiology 18, 1375–1402. https://doi.org/10.1089/ast.2017.1773.
Oremland, R.S., Stolz, J.F., 2003. The ecology of arsenic. Science 300, 939–944. https://doi.org/10.1126/science.1081903.
Osinski, G.R., et al., 2013. Impact-generated hydrothermal systems on Earth and mars. Icarus 224, 347–363. https://doi.org/10.1016/j.icarus.2012.08.030.
Palmer, P.T., Limero, T.F., 2001. Mass spectrometry in the U.S. space program: past, present, and future. J. Am. Soc. Mass Spectrom. 12, 656–675. https://doi.org/10.1016/S1044-0305(01)00249-5.
Pancost, R.D., Pressley, S., Coleman, J.M., Benning, L.G., Mountain, B.W., 2005. Lipid biomolecules in silica sinters: indicators of microbial biodiversity. Environ. Microbiol. 7, 66–77. https://doi.org/10.1111/j.1462-2920.2004.00686.x.
Parenteau, M.N., Jahnke, L.L., Farmer, J.D., Cady, S.L., 2014. Production and early preservation of lipid biomarkers in iron hot springs. Astrobiology 14, 502–521. https://doi.org/10.1089/ast.2013.1122.
Passos, L.S., de Freitas, P.N.N., Menezes, R.B., de Souza, A.O., da Silva, M.F., Converti, A., Pinto, E., 2023. Content of lipids, fatty acids, carbohydrates, and proteins in continental cyanobacteria: a systematic analysis and database application. Appl. Sci. 13, 3162. https://doi.org/10.3390/app13053162.
Pavlov, A.A., Vasilyev, G., Ostryakov, V.M., Pavlov, A.K., Mahaffy, P., 2012. Degradation of the organic molecules in the shallow subsurface of Mars due to irradiation by cosmic rays: organic matter and cosmic rays on mars. Geophys. Res. Lett. 39 https://doi.org/10.1029/2012GL052166 n/a-n/a.
Pavlov, A.A., McLain, H.L., Glavin, D.P., Roussel, A., Dworkin, J.P., Elsila, J.E., Yocum, K.M., 2022. Rapid radiolytic degradation of amino acids in the martian shallow subsurface: implications for the search for extinct life. Astrobiology. https://doi.org/10.1089/ast.2021.0166 ast.2021.0166.
Pietrogrande, M.C., Bacco, D., Chiereghin, S., 2013. GC/MS analysis of water-soluble organics in atmospheric aerosol: optimization of a solvent extraction procedure for simultaneous analysis of carboxylic acids and sugars. Anal. Bioanal. Chem. 405, 1095–1104. https://doi.org/10.1007/s00216-012-6592-4.
Prieto-Ballesteros, O., Kargel, J.S., Fairén, A.G., Fernández-Remolar, D.C., Dohm, J.M., Amils, R., 2006. Interglacial clathrate destabilization on Mars: possible contributing source of its atmospheric methane. Geology 34, 149–152. https://doi.org/10.1130/G22311.1.
Reinhardt, M., Goetz, W., Thiel, V., 2020. Testing flight-like pyrolysis gas chromatography–mass spectrometry as performed by the mars organic molecule analyzer onboard the ExoMars 2020 rover on Oxia Planum analog samples. Astrobiology 20, 415–428. https://doi.org/10.1089/ast.2019.2143.
Rimola, A., Sodupe, M., Ugliengo, P., 2019. Role of mineral surfaces in prebiotic chemical evolution. Silico Quantum Mechanical Studies, Life 9, 10. https://doi.org/10.3390/life9010010.
Robertson, C.E., Harris, J.K., Spear, J.R., Pace, N.R., 2005. Phylogenetic diversity and ecology of environmental Archaea. Curr. Opin. Microbiol. 8, 638–642. https://doi.org/10.1016/j.mib.2005.10.003.
Ruff, S.W., et al., 2011. Characteristics, distribution, origin, and significance of opaline silica observed by the Spirit rover in Gusev crater, Mars. J. Geophys. Res.: Planets 116. https://doi.org/10.1029/2010JE003767.

Rull, F., Veneranda, M., Manrique-Martinez, J.A., Sanz-Arranz, A., Saiz, J., Medina, J., Moral, A., Perez, C., Seoane, L., Lalla, E., Charro, E., Lopez, J.M., Nieto, L.M., Lopez-Reyes, G., 2022. Spectroscopic study of terrestrial analogues to support rover missions to Mars – a Raman-centred review. Anal. Chim. Acta 1209, 339003. https://doi.org/10.1016/j.aca.2021.339003.

Scheller, E.L., et al., 2022. Aqueous alteration processes in Jezero crater, Mars—implications for organic geochemistry. Science 378, 1105–1110.

Schmitt-Kopplin, P., Gabelica, Z., Gougeon, R.D., Fekete, A., Kanawati, B., Harir, M., Gebefuegi, I., Eckel, G., Hertkorn, N., 2010. High molecular diversity of extraterrestrial organic matter in Murchison meteorite revealed 40 years after its fall. Proc. Natl. Acad. Sci. USA 107, 2763–2768. https://doi.org/10.1073/pnas.0912157107.

Schon, S.C., Head, J.W., Fassett, C.I., 2012. An overfilled lacustrine system and progradational delta in Jezero crater, Mars: implications for Noachian climate. Planet. Space Sci. 67, 28–45. https://doi.org/10.1016/j.pss.2012.02.003.

Schuler, C.G., Havig, J.R., Hamilton, T.L., 2017. Hot spring microbial community composition, morphology, and carbon fixation: implications for interpreting the ancient rock record. Front. Earth Sci. 5. https://www.frontiersin.org/articles/10.3389/feart.2017.00097.

Sforna, M.C., et al., 2014. Evidence for arsenic metabolism and cycling by microorganisms 2.7 billion years ago. Nat. Geosci. 7, 811–815. https://doi.org/10.1038/ngeo2276.

Sharma, S., et al., 2023. Diverse organic-mineral associations in Jezero crater, Mars. Nature 1–9.

Shiea, J., Brassel, S.C., Ward, D.M., 1991. Comparative analysis of extractable lipids in hot spring microbial mats and their component photosynthetic bacteria. Org. Geochem. 17, 309–319. https://doi.org/10.1016/0146-6380(91)90094-Z.

Squyres, S.W., et al., 2008. Detection of silica-rich deposits on mars. Science 320, 1063–1067. https://doi.org/10.1126/science.1155429.

Stack-Morgan, K.M., et al., 2023. Sedimentology and stratigraphy of the lower delta sequence, Jezero Crater, mars. In: 54th Lunar and Planetary Science Conference. Lunar and Planetary Institute, The Woodlands (Texas), United States, p. 1422. https://hal.science/hal-04052338. (Accessed 11 September 2023).

Szopa, C., et al., 2020. First detections of dichlorobenzene isomers and trichloromethylpropane from organic matter indigenous to mars mudstone in Gale Crater, mars: results from the sample analysis at mars instrument onboard the curiosity rover. Astrobiology 20, 292–306. https://doi.org/10.1089/ast.2018.1908.

Teece, B.L., Guido, D.M., Campbell, K.A., Van Kranendonk, M.J., Galar, A., George, S.C., 2022. Exceptional molecular preservation in the late jurassic claudia palaeo-geothermal field (deseado massif, patagonia, Argentina). Org. Geochem. 173, 104504 https://doi.org/10.1016/j.orggeochem.2022.104504.

Teece, B.L., Havig, J.R., George, S.C., Hamilton, T.L., Baumgartner, R.J., Hartz, J., Van Kranendonk, M.J., 2023. Biogeochemistry of recently fossilized siliceous hot spring sinters from Yellowstone, USA. Astrobiology 23, 155–171. https://doi.org/10.1089/ast.2022.0012.

Thomazo, C., Pinti, D.L., Busigny, V., Ader, M., Hashizume, K., Philippot, P., 2009. Biological activity and the Earth's surface evolution: insights from carbon, sulfur, nitrogen and iron stable isotopes in the rock record. Comptes Rendus Palevol 8, 665–678. https://doi.org/10.1016/j.crpv.2009.02.003.

Tomečková, L., Tomčala, A., Oborník, M., Hampl, V., 2020. The lipid composition of euglena gracilis middle plastid membrane resembles that of primary plastid Envelopes1. Plant Physiol. 184, 2052–2063. https://doi.org/10.1104/pp.20.00505.

Vago, J.L., et al., 2017. Habitability on early mars and the search for biosignatures with the ExoMars rover. Astrobiology 17, 471–510. https://doi.org/10.1089/ast.2016.1533.

van der Meer, M.T., Schouten, S., de Leeuw, J.W., Ward, D.M., 2000. Autotrophy of green non-sulphur bacteria in hot spring microbial mats: biological explanations for isotopically heavy organic carbon in the geological record. Environ. Microbiol. 2, 428–435. https://doi.org/10.1046/j.1462-2920.2000.00124.x.

van der Meer, M.T.J., et al., 2010. Cultivation and genomic, nutritional, and lipid biomarker characterization of Roseiflexus strains closely related to predominant in situ populations inhabiting Yellowstone hot spring microbial mats. J. Bacteriol. 192, 3033–3042. https://doi.org/10.1128/JB.01610-09.

Veneranda, M., Lopez-Reyes, G., Manrique-Martinez, J.A., Sanz-Arranz, A., Medina, J., Pérez, C., Quintana, C., Moral, A., Rodríguez, J.A., Zafra, J., Nieto Calzada, L.M., Rull, F., 2021. Raman spectroscopy and planetary exploration: testing the ExoMars/RLS system at the Tabernas Desert (Spain). Microchem. J. 165, 106149 https://doi.org/10.1016/j.microc.2021.106149.

Vinçon-Laugier, A., Cravo-Laureau, C., Mitteau, I., Grossi, V., 2017. Temperature-dependent alkyl glycerol ether lipid composition of mesophilic and thermophilic sulfate-reducing bacteria. Front. Microbiol. 8. https://www.frontiersin.org/articles/10.3389/fmicb.2017.01532.

Visscher, P.T., et al., 2020. Modern arsenotrophic microbial mats provide an analogue for life in the anoxic Archean. Commun Earth Environ 1, 1–10. https://doi.org/10.1038/s43247-020-00025-2.

Vogel, C., Heister, K., Buegger, F., Tanuwidjaja, I., Haug, S., Schloter, M., Kögel-Knabner, I., 2015. Clay mineral composition modifies decomposition and sequestration of organic carbon and nitrogen in fine soil fractions. Biol. Fertil. Soils 51, 427–442. https://doi.org/10.1007/s00374-014-0987-7.

Volkman, J.K., 2006. Lipid markers for marine organic matter. In: Volkman, J.K. (Ed.), Marine Organic Matter: Biomarkers, Isotopes and DNA. Springer, Berlin, Heidelberg, pp. 27–70. https://doi.org/10.1007/698_2_002.

Waldrop, H.A., Pierce, K.L., 1975. Surficial geologic map of the madison junction quadrangle. Yellowstone National Park, Wyoming, IMAP. https://doi.org/10.3133/i651.

Webster, C.R., et al., 2015. Mars methane detection and variability at Gale crater. Science 347, 415–417. https://doi.org/10.1126/science.1261713.

Weerkamp, A., Heinen, W., 1972. Effect of temperature on the fatty acid composition of the extreme thermophiles, Bacillus caldolyticus and Bacillus caldotenax. J. Bacteriol. 109, 443–446. https://doi.org/10.1128/jb.109.1.443-446.1972.

Wen, P., Wang, Y., Huang, W., Wang, W., Chen, T., Yu, Z., 2022. Linking microbial community succession with substance transformation in a thermophilic ectopic fermentation system. Front. Microbiol. 13, 886161 https://doi.org/10.3389/fmicb.2022.886161.

Wilhelm, M.B., et al., 2017. Xeropreservation of functionalized lipid biomarkers in hyperarid soils in the Atacama Desert. Org. Geochem. 103, 97–104. https://doi.org/10.1016/j.orggeochem.2016.10.015.

Williams, A.J., et al., 2019. Recovery of fatty acids from mineralogic mars analogs by TMAH thermochemolysis for the sample analysis at mars wet chemistry experiment on the curiosity rover. Astrobiology 19, 522–546. https://doi.org/10.1089/ast.2018.1819.

Williams, A., et al., 2021a. Results from the TMAH wet chemistry experiment on the sample analysis at mars (SAM) instrument onboard NASA's curiosity rover, 43, 1939.

Williams, A.J., Craft, K.L., Millan, M., Johnson, S.S., Knudson, C.A., Juarez Rivera, M., McAdam, A.C., Tobler, D., Skok, J.R., 2021b. Fatty acid preservation in modern and relict hot-spring deposits in Iceland, with implications for organics detection on mars. Astrobiology 21, 60–82. https://doi.org/10.1089/ast.2019.2115.

Yuen, G.U., Kvenvolden, K.A., 1973. Monocarboxylic acids in murray and murchison carbonaceous meteorites. Nature 246, 301–303. https://doi.org/10.1038/246301a0.

Zeikus, J.G., Ben-Bassat, A., Ng, T.K., Lamed, R.J., 1981. Thermophilic ethanol fermentations. In: Hollaender, A., Rabson, R., Rogers, P., Pietro, A.S., Valentine, R., Wolfe, R. (Eds.), Trends in the Biology of Fermentations for Fuels and Chemicals. Springer US, Boston, MA, pp. 441–461. https://doi.org/10.1007/978-1-4684-3980-9_26.

Zeng, Y.B., Ward, D.M., Brassell, S.C., Eglinton, G., 1992. Biogeochemistry of hot spring environments: 2. Lipid compositions of Yellowstone (Wyoming, U.S.A.) cyanobacterial and Chloroflexus mats. Chem. Geol. 95, 327–345. https://doi.org/10.1016/0009-2541(92)90020-6.